WAGENINGEN UNIVERSITY
MASTER'S THESIS

Climate Active Trace Gas Exchange in the Arctic with a focus on Dimethyl Sulphide: a 1-D modelling approach

Author: Smriti Tiwari
Supervisor: Dr. Laurens Ganzeveld
Department of Meteorology and Air Quality

May 30, 2019

Document Title	Climate Active Trace Gas Exchange in the Arctic with a focus on Dimethyl Sulphide: 1-D modelling approach. *Master's thesis for the master program Climate Studies at Wageningen University*
Date	May 30, 2019
Author	Smriti Tiwari tsmriti97@gmail.com
Assessment committee	Dr. Laurens Ganzeveld Prof. dr. Maarten Krol
Wageningen University	Department of Meteorology and Air Quality

Abstract

The Arctic region is seeing unprecedented warming due to the occurrence of amplifying feedback mechanisms such as the ice-albedo feedback mechanism. This can have implications for climate-active trace gas (e.g., carbon dioxide, methane, ozone) exchange in this region which, in turn, further influence the Arctic climate. In this study, we aimed to further identify the role of biogeochemistry involved in the exchange of Dimethyl sulphide (DMS) and Carbon dioxide (CO_2) from the sea ice/ocean to the atmosphere. Through a literature review we identified the main processes involved in the production and consumption of the gases. Further, we also implemented a mechanistic sea-ice/ocean surface layer DMS cycle model in a simplified box modelling system to obtain seasonally varying sea-atmosphere DMS fluxes for a measurement site in the North Canadian Arctic. These fluxes were then used as input for a 1-D meteorological and atmospheric chemistry model to simulate atmospheric DMS mixing ratios. The review mainly indicates that the sea ice and underlying water column DMS production and consumption processes have been quantified to some extent. However, there is still lack of data, for example, on activity of prevalent enzymes (DMSPlyase), zooplankton grazing rate measurements and the impact of climate change on DMS release from the sea ice/ocean. There is also uncertainty in the representation of these sea-ice DMS production and consumption processes in models due to lack of in-situ measurements. The emissions of DMS from the underlying water column into the atmosphere varies by season and the atmospheric mixing ratios depend not only on chemical oxidation efficiency but also on temperature and boundary layer mixing. Seasonal contrasts in all these processes result in simulated maximum DMS mixing ratios up to 3-5 ppbv in late Spring, which seem to be unrealistically high. However, this cannot be further corroborated due to missing measurements on specific features such as a very shallow atmospheric inversion layer. These results stress the need for long-term measurement of both the ocean/sea ice and atmospheric cycling of DMS (and other climate-active trace gases) to improve our understanding of their role in the Arctic climate.

Table of Contents

1. Introduction

The Arctic region is the northernmost region of our planet, most commonly defined as the area north of the Arctic circle (see Figure 1). It is a primarily a large ocean surrounded by landmass on all sides. It experiences extreme weather conditions: cold and dark winters and summers with perpetual sunshine. The Arctic region is a hotspot for climate research today due to the drastic changes that are being observed in the region and the incomplete understanding of their consequences (Barnes and Screen 2015, Ma, Zhu et al. 2018). The most important phenomenon that has been influencing the region's climate is Arctic amplification. It is defined as the enhanced and accelerated warming of the Arctic when compared to the lower latitudes for the same amount forcing by the greenhouse gases present in the atmosphere (Serreze and Francis 2006). Altered sea ice albedo and its impact on Earth's energy and radiative balance, and extreme weather in the mid-latitudes are a few of the studied impacts of this amplification (Francis and Vavrus 2012, Coumou, Di Capua et al. 2018, Kim, Kim et al. 2019).

Figure 1 Map of Arctic region. Reprinted from Arctic Circle, In Wikipedia, n.d., Retrieved September 26, 2018, from https://en.wikipedia.org/wiki/Arctic_Circle. Made available in public domain by CIA World Fact Book

The influence of climate active trace gases, such as CO_2, on the Arctic climate has been studied to a limited extent. This is largely due to the scarcity of in-situ flux measurements because of harsh and often unnavigable conditions (Mortenson, Hayashida et al. 2017, Vihma, Uotila et al. 2018). The few available ocean-sea ice- atmosphere exchange measurements are generally point measurements taken during the summer months. Hence, they cannot be generalized over the entire area or year. Further, for a long time it was believed that sea ice is impermeable to any gaseous exchange (Tedesco and Vichi 2014). However, it has been observed that sea ice is permeable to gases at temperatures above -15°C and certain salinity conditions (Delille, Vancoppenolle et al. 2014, Kotovitch, Moreau et al. 2016). This has led to increased efforts to understand the prevalent biogeochemistry that results in the exchange of these gases from the ocean to the atmosphere and vice versa (Kotovitch, Moreau et al. 2016, Hayashida, Steiner et al. 2017).

The Multidisciplinary drifting Observatory for the Study of Arctic Climate (MOSAiC) project is an upcoming scientific effort to increase the understanding of the role of climate-active trace gas exchange in the Arctic climate change. As a part of the project, continuous measurement of gas fluxes and meteorological parameters, among other measurements, will be conducted for 13-months along the drift track of the German Research Vehicle, Polarstern (n.d.). These measurements will be analysed using process-based models of ocean biogeochemistry, its physical and dynamical drivers and atmospheric cycling. As a contribution to the MOSAiC project, two research projects (one funded by the USA National Science Foundation and another one by the Dutch Science foundation) will focus on measurements and modelling of climate-active trace gas exchange between the Arctic ocean/sea ice/atmosphere interface. The

four gases that will be measured are- CO_2, Methane (CH_4), Ozone (O_3) and Dimethyl Sulphide (DMS).

This thesis is a precursory study to the MOSAiC campaign and focuses primarily on DMS. This gas was chosen as it is a highly relevant climate-active trace gas in the remote Arctic and there is a need to understand the inherent mechanisms involved in its production, consumption and role in the Arctic atmosphere and climate (Hayashida, Steiner et al. 2017, Abbatt, Leaitch et al. 2018). In addition, we also consider in the review component of this study, the cycling and exchange of CO_2. This is because it shares a mutual component of ocean/sea ice biogeochemistry with the DMS cycling and exchange. The exchange of CH_4 and O_3 are not considered in this study also due to time limits but will be the focus of follow-up studies as a contribution to MOSAiC.

Consequently, this thesis study aims to answers the following research questions.

1. **What are the relevant biogeochemical and physical processes important for exchange of DMS and CO_2 in the Arctic?**

2. **What are the main uncertainties involved in this exchange of DMS and CO2?**

3. **What is the temporal variability in atmospheric DMS concentrations and cycling as a function of ocean-sea ice cycling, meteorology and atmospheric chemistry?**

The above questions will be answered by aggregating the available knowledge on the biogeochemistry involved in the production of DMS and CO_2 through a literature review in Chapter 2. This is important because on regional scales, like the Arctic, these processes play a crucial role but our knowledge of the involved processes is limited (Steiner, Deal et al. 2016). In Chapter 3, we present the implementation and application of a 1-D DMS model for the cycling and exchange between the ocean/sea ice/atmosphere, originally developed by Hayashida, Steiner et al. (2017), in a box model software package called SMART (Simulation and Modelling Assistant for Research and Training). This model considers DMS production in the sea-ice and underlying ocean, and ultimately calculates the flux to the atmosphere but does not consider the resulting DMS cycling in the atmosphere. Implementation in the SMART model enables us to closely examine the involved biogeochemistry and identify the most sensitive parameters. We then use the DMS flux output from the SMART model experiments as input for simulations with the Single Column Model (SCM) (Ganzeveld, Lelieveld et al. 2002, Ganzeveld, Eerdekens et al. 2008) a 1-D meteorology-atmospheric chemistry model. From this step, we obtain the DMS mixing ratios which we can then compare to observations and draw preliminary conclusions regarding the potential implications for the Arctic climate. These results are presented in Chapter 4. In Chapter 5, the results are discussed and recommendations are made regarding future focus on crucial processes and the most sensitive parameters involved in this ocean/sea ice/atmosphere cycling and exchange of DMS.

2. Literature Review

In this section of the thesis we provide a review of the available knowledge on the cycling and exchange of the climate-active trace gases, DMS and CO_2 considered relevant for the Arctic region. We aim with this review to highlight the areas where research is needed to improve our understanding and model representation to assess the role of climate-active trace gas exchange in Arctic climate change.

2.1. Dimethyl sulphide (DMS)

DMS is a volatile compound produced in marine environments through the biological activity of phytoplankton. Its role in the climate has been investigated for over three decades. It is postulated to affect the climate through its role in cloud formation either by the formation of sulphate aerosols or as a precursor to cloud condensation nuclei (CCN). In a landmark study in 1987, Charlson, Lovelock, Andreae and Wallace proposed the CLAW (after their names) hypothesis reflecting that the release of DMS resulted in the altered albedo of clouds and hence, a compensating effect on the Earth's climate (Charlson, Lovelock et al. 1987) (see Figure 2). However, the relevance of this hypothesis for the global climate is still uncertain (Halloran, Bell et al. 2010, Stefels, van Leeuwe et al. 2018). Assessing the relevance of this feedback mechanism for the Arctic is hampered by a lack of sufficient in-situ measurements. Further, our understanding of the biogeochemistry involved in the production of DMS within the sea-ice and open Arctic ocean is still incomplete (red box in Figure 2). In the sections below, we will discuss the cycling of DMS in the sea-ice, open ocean and atmosphere, respectively. Lastly, we will discuss its role in the climate and possible impacts of climate change.

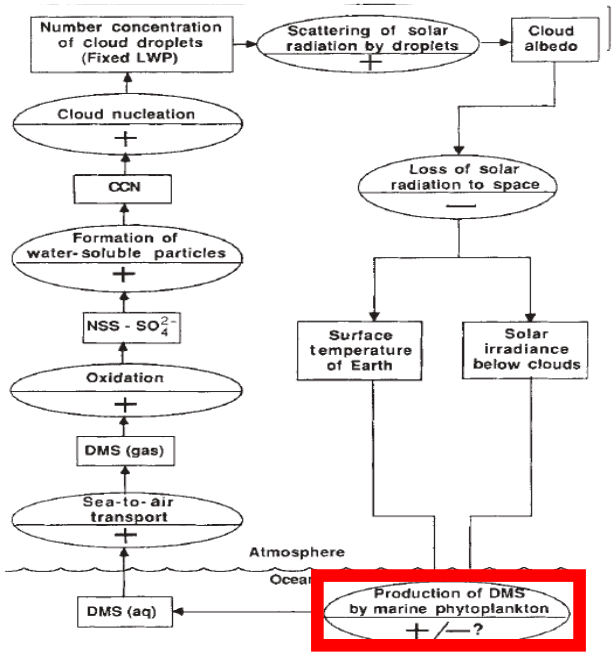

Figure 2 Schematic representation of the CLAW hypothesis. From "Oceanic phytoplankton, atmospheric sulphur, cloud albedo and climate" by R.J. Charlson et al., 1987, Nature, 326, pg 65., Copyright by Springer Nature 1987. Adapted with permission.

2.1.1. Sea-ice Sulphur cycle

DMS is produced in the marine ecosystem primarily in the form of its precursor Dimethyl Sulphoniopropionate (DMSP). The latter is produced by phytoplankton and sea ice algae. It exists in two different phases: particulate DMSP (DMSPp) found within the algal cells and dissolved DMSP (DMSPd) found outside the cell. The different chemical states, particulate and dissolved, have different physical properties and ecological roles in the cycling process (Hayashida, Steiner et al. 2017). In earlier studies of the polar region, only total DMSP (DMSPp + DMSPd) was considered due to insufficient sample observations. However, Galindo, Levasseur et al. (2014) determined total DMSP as well as DMSPd concentrations in sea-ice and water samples from the Canadian Arctic Archipelago, using the ice melt technique. In this method, ice core samples were collected and allowed to melt in sea-water, as measurements were taken, to minimize osmotic stress. Other methods that have been used to carry out measurements include, the dry crushing technique to restrict the conversion of DMSP to DMS and the addition of stable isotopes to the samples to monitor the conversion processes (Stefels, Carnat et al. 2012). Figure 3 shows the main processes involved in conversion of DMSP to DMS in the sea-ice and underlying water column.

Particulate DMSP is a well-known compound produced in several phytoplankton species, due to its role in osmoregulation, and also as a cryoprotectant and anti-oxidant (Stefels, Steinke et al. 2007, Galindo, Levasseur et al. 2014). Further, it is reported to aid cell metabolism as a solute in cold conditions (Stefels, Steinke et al. 2007). Lee, De Mora et al. (2001) reported DMSPp concentrations of 8.66-987 nmol L^{-1} in the bottom sea ice (lowest 2cm) between April- June in the North Water region of northern Baffin Bay, Canada. Much higher values (~5000 nmol L^{-1}) were reported by Galindo, Levasseur et al. (2014) in their observations for Resolute passage, in the same season. This large discrepancy between measurements could be due to improved techniques but may also be due to the changed climate of the Arctic. DMSPp is converted to DMSPd primarily by exudation from algal cells, lysis of cells due to senescence or viral attack (Stefels, Steinke et al. 2007). The exudation process is species specific and can be influenced by salinity, temperature and nutrient limitation (Stefels, Steinke et al. 2007). Cell lysis is triggered in nutrient limited conditions and has been reported to be the source for particulate DMSP in the oceanic surface layer when the sea-ice melts and algal blooms are flushed into the underlying water (Stefels, Carnat et al. 2012, Hayashida, Steiner et al. 2017). Although not shown in Figure 3, DMSPp is also released into the under-lying water column due to brine drainage (Galindo, Levasseur et al. 2014, Hayashida, Steiner et al. 2017). The understanding of this process is not complete and hence its parameterizations in models is poorly constrained.

A fraction of the DMSPd, being formed as a result of the above processes, is converted to DMS through the action of DMSP-lyase. Although it is a crucial enzyme, little is known about its production and regulation in algal bodies, especially those found in sea-ice (Stefels, Steinke et al. 2007). DMSPd is also consumed and converted to DMS by the bacterial population present in the sea-ice. Further, some of it is released into the underlying water column. The modelling study by Hayashida, Steiner et al. (2017) found that bacterial consumption dominated the DMSPd to DMS conversion, with smaller rates of loss by lyase activity and release into water.

A part of the DMS formed is converted to Dimethyl Sulphoxide (DMSO) by photolysis. The rate of this process is mainly determined by ambient light conditions, especially in the UV region.

The fate of the compounds released into the underlying water column is discussed in the section below.

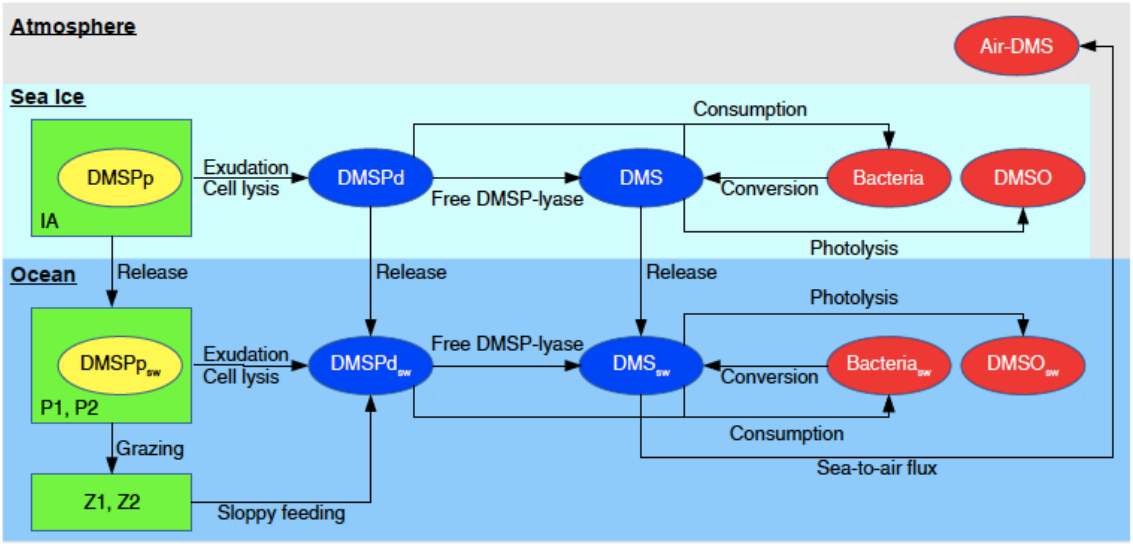

Figure 3 Schematic representation of the sea-ice and oceanic components of the DMS cycle in the Arctic region. From "Implications of sea-ice biogeochemistry for oceanic production and emissions of dimethyl sulfide in the Arctic" by H. Hayashida et al., 2017, Biogeosciences, 14, 3132.CC-BY 3.0.

2.1.2. Ocean Sulphur Cycle

The particulate DMSP in the underlying water column ($DMSPp_{sw}$) is found in the phytoplankton. It is converted to dissolved DMSP in sea water ($DMSPd_{sw}$) by processes like exudation and cell lysis, as discussed in the previous section. Additionally, grazing by zooplanktons on the phytoplankton also results in the release of $DMSPd_{sw}$.. Stefels, Steinke et al. (2007) reviewed the role of micro-, meso- and macro-zooplankton in this conversion and release process and report that 20-70% of the ingested DMSPp was converted into DMSPd by micro-zooplankton. These numbers are valid under the assumption that selective grazing does not occur and all the DMSPp is found within the algal cells. However, since DMSPp is also found within the micro-zooplanktons, these percentages may be an overestimation (Stefels, Steinke et al. 2007). The grazing by larger zooplanktons such as krill, is termed as sloppy feeding. This process results in physical damage of the phytoplankton and leads to the release of $DMSPd_{sw}$. However, due to insufficient data on zooplankton and grazing it is difficult to draw concrete conclusions and formulate parameterisations for sloppy feeding in the Arctic region (Stefels, Steinke et al. 2007, Hayashida, Steiner et al. 2017).

$DMSPd_{sw}$, formed by the processes described above, is converted to DMS by bacterial consumption and degradation along with the release of an acrylate ion. The breakdown is caused by the DMSP lyase found inside the bacteria. However, presence of DMSP-cleaving enzymes cannot be seen as a proxy for DMS production (Stefels, Steinke et al. 2007). The mechanism for this breakdown is similar to the algal breakdown and hence it is difficult to differentiate between them during sampling studies. A competing degradation pathway is demethylation/demethiolation which does not lead to the formation of DMS but in quantitative terms, is a major pathway of $DMSPd_{sw}$

degradation (Stefels, Steinke et al. 2007). Kiene, Linn et al. (2000) hypothesize that the bacterial demand of sulphur determines the amount of $DMSPd_{sw}$ degraded into DMS. Stefels, Steinke et al. (2007) support this by stipulating that in younger algal blooms the sulphur demand is low and hence more DMS is released. On the other hand, in mature blooms, the $DMSPd_{sw}$ is degraded by demethylation pathway to meet the sulphur demand.

Apart from the release into the atmosphere, DMS is removed from the sea water also by bacterial consumption and photolysis. It is also oxidized into $DMSO_{sw}$ by a large variety of micro-organisms especially those that oxidize sulphur and ammonia (Stefels, Steinke et al. 2007). In contrast, laboratory experiments have shown that $DMSO_{sw}$ is also reduced by bacteria colonies to actually form DMS. However, this has only been measured in the Antarctic (see Asher, Dacey et al. (2011) and needs to be supplemented with more observations to be included in model developments. Bacterial consumption and conversion are estimated to account for 50-80% of the DMS loss (Stefels, Steinke et al. 2007). Photolysis, similarly, also depends on the DMS concentrations and occurs between the wavelengths of 380-460 nm (Stefels, Steinke et al. 2007). Further, Stefels, Steinke et al. (2007) review that photolysis is mediated by 1) coloured dissolved organic matter and 2) depends largely linearly on nitrate concentration, wavelength and temperature. This is also supported by the findings of Taalba, Xie et al. (2013) in their evaluation of photolysis in the Canadian Arctic waters. Given these several influencing factors, photolysis cannot be parameterized easily. Additionally, Simó and Pedrós-Alió (1999) found that in the North Atlantic, DMS photolysis was the dominant removal process for clear skies conditions and reduced water column mixing conditions. In contrast, bacterial consumption dominated when there were cloudy skies and enhanced vertical mixing in the water column. During storms, they found that the rate of DMS flux from sea to air was equivalent to loss through bacterial consumption. Hence, measurement campaigns, like MOSAiC covering a full year of measurements, most likely also under such varying conditions, can help to further validate these findings and facilitate better representation in models.

2.1.3. Atmospheric Sulphur cycle

Once the DMS is released into the atmosphere, it is oxidized through photolysis and by agents like O_3 and the hydroxyl radical (OH) to form Methane Sulphonic Acid (MSA), DMSO and SO_2. These oxidation products form the largest biological source of natural sulphur and non-sea-salt-sulphate ($nss\text{-}SO_4^{2-}$) aerosols (Hoffmann, Tilgner et al. 2016). DMS is also oxidized by Hypobromite (BrO^-) to form DMSO which is further oxidized to form MSA (Breider, Chipperfield et al. 2010). Similarly, the SO_2 formed is oxidized to H_2SO_4 which can act as an aerosol or condense upon existing aerosols.

DMS concentrations in the Arctic atmosphere were first obtained using airborne measurements, as elaborated in Ferek, Hobbs et al. (1995). In June 1990, the DMS concentrations ranged between 0.001-0.283 ppbv and SO_2 was found to be <0.001-0.982 ppbv at various heights and locations near Barrow, Canada. In April 1992, the DMS concentrations were sometimes below the detection limit and reached the maximum value of 0.0096 ppbv and SO_2 was found to be <0.001- 0.278 ppbv near Prudhoe bay and Barrow. It is important to indicate here that these measurements were carried out over an entire month at different locations, heights and weather conditions. Hence, these factors should be carefully considered before any conclusions are drawn

from these measurements. More recent measurements by Mungall, Croft et al. (2016) have shown mixing ratios of up to 1.1 ppbv in July and August, 2014. The highest reported concentration for the Arctic is 1.8 ppbv in July and August, 2016 (Abbatt, Leaitch et al. 2018).

The release of DMS into the atmosphere, as is clear from the reviewed information on sea-ice and ocean water production and destruction processes, is seasonal. The highest peaks are seen during the Arctic summer (June – August). One of the earliest studies to clearly demonstrate this peak fluxes and concentrations was conducted by Li and Barrie (1993). They measured aerosol concentrations and the contribution by MSA, SO_4^{2-} to these aerosol fluxes at Alert, Nunavut, Canada between 1980-1990. Using the measurements and sulphur isotope composition method, they found that in summer, 25-30% of sulphate aerosols were produced from biogenic sources such as DMS and MSA. In winter, the inferred biogenic contribution was smaller, ~14%, but also with a larger uncertainty. More recently, a modelling study by Yang, Wang et al. (2018) used sulphur tagging techniques to determine the source of sulphate aerosols in the Arctic. They found that natural sources, including DMS, contributed to 50% of the near-surface concentrations and 6% of the annual mean sulphate column burden. The role of these aerosols in the Arctic climate is discussed below.

2.1.4. Role in Arctic Climate

The role of DMS in the climate has been studied for a long time. After the CLAW hypothesis was proposed, several studies have looked at the DMS contribution to aerosol formation and hence CCN. It has been found that sulphate aerosols formed do lead to an increase in the number of Aitken mode particles (diameter < 0.1μm) and also change the hygroscopicity of existing sulphate particles (Schwinger, Tjiputra et al. 2017). These Aitken mode particles do not usually directly contribute to CCN formation. Nevertheless, their growth, by either condensation on other particles or coagulation, can form the main source of DMS- derived CCN in remote areas, such as the Arctic (Mahmood, von Salzen et al.).

In contrast to the above studies, Leaitch, Sharma et al. (2013) do report new particle formation associated with MSA in summertime at Alert, Nunavut, Canada. They use observation and model results and show that DMS was the source of CCN for nearly 50% of the days in June-July, 2011. They attribute this to a lack of anthropogenic sources during this season which renders biogenic sources, like DMS, to play a significant role in in Arctic climate. However, how this affects Arctic climate, still needs to be assessed since in clean atmospheres CCN formation associated with the presence of DMS may increase longwave warming by clouds but otherwise may lead to shortwave cooling (Abbatt, Leaitch et al. 2018).

2.1.5. Impact of Climate Change

A reduction in sea ice and increased open water area resulting in increased primary production and hence, DMS production, is an intuitive cause-effect relationship. However, despite several studies, it is still difficult to estimate DMS emissions and the impact of sea-ice melt on these emissions (Mahmood, von Salzen et al. 2018). A correlation between sea ice melt, primary production and MSA release has been reported by Sharma, Chan et al. (2012) and Becagli, Lazzara et al. (2016). However,

this relation is influenced by several factors and hence there are discrepancies between studies. For example, Levasseur (2013) predicts an increase in emission due to enhanced open water areas and melt ponds. However, they acknowledge its dependence on the underlying biological processes and their representation in current models. Mahmood, von Salzen et al. (2018) also predict enhanced DMS emissions from the Arctic region in 2050 compared to 2000 but report that this does not necessarily result in an increase in sulphate aerosols concentrations due to increased amount of wet deposition. On the other hand, Schwinger, Tjiputra et al. (2017) report a reduction in DMS release due to ocean acidification and nutrient limitation. This is also supported by the findings of Archer, Kimmance et al. (2013) who report a decrease in DMS release but an increase of DMSP concentrations under low pH conditions. They did not find a clear explanation for this anomaly but concluded that it could be due to increased demand of DMSP by bacteria or reduced free-lyase activity in more acidic ocean. An increase in DMSP was also reported by (Stefels, Steinke et al. 2007) on long term scales for the extreme conditions found in the Arctic. In further contrast, Hopkins, Nightingale et al. (2018), from their microcosm studies report that the release of Arctic DMS is resilient to change in ocean acidification, at least on shorter time scales. and enable coherence between results of the link between climate-related drivers and ocean-sea ice-atmosphere DMS cycling

Regarding the role of DMS and its oxidation products in the formation of CCN, the studies are just as varied (Abbatt, Leaitch et al. 2018). The latest study by Mahmood, von Salzen et al. (2018) using the Canadian Center for Climate Modelling and Analysis Atmospheric Model (CanAM4.3) found cloud radiative forcing to be proportional to surface sea water DMS concentrations Hence, they propose that increased DMS emissions could lead to increased aerosol nucleation rates and hence cloud droplet number concentration. This is turn could alter the cloud albedo and finally result in negative feedback on the climate. A more detailed discussion of the impact of Arctic aerosol and its link to CCN can be found in Abbatt, Leaitch et al. (2018).

This large discrepancy in our understanding of the link between climate-related drivers and ocean-sea ice-atmosphere DMS cycling highlights the need for studies like MOSAiC where year-long measurements can help us improve model parameterizations

2.1.6. Physical processes relevant for DMS

As is clear from the above discussion, DMS production is highly dependent on the nature of the environment available for the growth of the bacteria, algae, phytoplankton and zooplankton. However, the physical factors also regulate DMSP and DMS regulation production. For example, DMS and MSA concentrations have been found to coincide with onset of sea-ice melt (Li and Barrie 1993). The nature of sea ice cover (first year or multiyear ice), seasonal ice extent, marginal ice zones, melt ponds (Abbatt, Leaitch et al. 2018) are the main factors influencing DMS production and release. Furthermore, under-ice water, melt ponds and marginal ice zones have also been found to be hotspots for DMS production (Ghahremaninezhad, Norman et al. 2017) but their potential influence on the future Arctic climate is less studied (Abbatt, Leaitch et al. 2018).

With MOSAiC, it is hoped that these gaps in knowledge can be fulfilled and hence, we can obtain improved understanding of the role of DMS in the changing Arctic climate.

2.2. Carbon Dioxide (CO2)

Carbon dioxide is a well-known, potent greenhouse gas. Anthropogenic activities have caused a steady rise in CO_2 concentrations in the atmosphere since the industrial revolution. The Arctic region has experienced significant impacts due to this rise. This is evident from the decreasing sea ice cover extent derived from satellite data and is attributed to the phenomenon of Arctic amplification as discussed before. The reduced ice extent has the potential to have widespread implications for the oceanic uptake of CO_2 but it is not free of uncertainties (Parmentier, Christensen et al. 2013). In the review, we focus on the primary production in the sea ice and open ocean and the net uptake or release of CO_2 by these zones.

2.2.1. Sea ice interactions

Primary production within Arctic sea ice is carried out by algae which are predominantly found in the bottom few centimetres of the sea ice (Galindo, Levasseur et al. 2014). This is one of the ways CO_2 is taken up by the sea ice apart from other processes elaborated upon in Søren, Bendtsen et al. (2011). Given their habitat, the algae are adapted to low light conditions but have still been found to contribute 4-26% to the total primary production in seasonally ice covered regions (Gradinger 2009). This is because sea ice algae can grow up to a biomass of 1000 mg Chl a $m^{-3,}$ which is nearly two orders of magnitude larger compared to the phytoplankton biomass present in the underlying water column (Galindo, Levasseur et al. 2014). The rate of primary production has been mainly measured and modelled as a function of chlorophyll-a concentrations, nutrient and light availability (Lavoie, Denman et al. 2005). This production is primarily active in the early spring, between March – May while the temperatures are still low, and there is sufficient snow. Using a 1-D model, Lavoie, Denman et al. (2005) show that at the onset of the bloom, the algae are limited by light. In the intermediate period, the dependency shifts between light and nutrient limited regimes and towards the end, they become nutrient limited. Further, they find that melting of the snow cover over the ice leads to the end of the bloom and hence it acts as a control of the length of a bloom. This is because of melting of the snow cover triggers sea ice algal loss due to 1) the enhanced melting rate of the bottom ice and 2) a decrease in ice algal growth due to meltwater formation. Under these conditions, it can be expected sea ice algal production may reduce due to enhanced snow melt in a warmer Arctic climate. One additional finding of these studies with 1-D modelling system by Mortenson, Hayashida et al. (2017) was that ice algal growth limited the nutrient availability to the phytoplankton present in the underlying ocean surface layer and hence controlled their growth and development.

Given the primary production in sea ice, there is an observed seasonal trend of CO_2 influx from the atmosphere to sea ice in summer and CO_2 release to the atmosphere during winter (Nomura, Yoshikawa-Inoue et al. 2006, Moreau, Vancoppenolle et al. 2015, Kotovitch, Moreau et al. 2016). In observations carried out over fast ice in the Buror-Khaya Gulf, Laptev sea during summer, the partial pressure of CO_2 (pCO_2) was found to be negative (Semiletov, Makshtas et al. 2004). Hence, making it a sink for atmospheric CO_2. In winter, the pCO_2 was found to be positive as this is an area with high coastal erosion. They reported the summer time absorption to be roughly close to 40 Mt C per year and the winter time release to be in the range of 4-40 Mt C per year.

A study by Kotovitch et al. (2016) combined mesocosm (chambers for the formation of artificial ice) measurements and modelling experiments to understand CO_2 uptake and loss. The mesocosm showed uptake of atmospheric CO_2 during ice formation (average flux rate of 0.2 mmol m^{-2} d^{-1}) and emissions during melting of sea ice (average flux rate of 0.24 mmol m^{-2} d^{-1}). The modelling experiments also showed uptake and release of CO_2 in the same direction as seen in the mesocosms but the magnitude of the flux was highly variable. They also conclude that the observed sea ice-air flux values can only be explained by the inclusion of outgassing of CO_2 bubbles along with diffusion during ice formation although it has not been so far observed in field measurements. Similarly, Moreau, Vancoppenolle et al. (2015) explored the main factors influencing CO_2 dynamics within the sea ice using a 1-D thermodynamic model and ice-tank experiments for Barrow, Alaska. One of their main conclusions was that eddy covariance measured CO_2 fluxes over sea ice could not be explained by direct diffusion but also involves other process such as storage in snow cover, release from leads, etc.

Another source of CO_2 in the sea ice could be precipitation of $CaCO_3$ crystals during ice formation as has been observed in laboratory experiments (Papadimitriou, Kennedy et al. 2004). This may further concentrate the brine solutions and facilitate the expulsion of CO_2 bubbles (see section 2.2.3) but little evidence of this has been found in natural sea-ice conditions. For the Arctic region, Søren, Bendtsen et al. (2011) provided an estimate of CO_2 flux from the atmosphere into the sea ice of -14 TgC yr^{-1} when $CaCO_3$ precipitation in the sea ice was not considered. However, when this process was considered, this flux increased up to -31 TgC yr^{-1}. This further highlights the need for measurement campaigns like MOSAiC where such uncertain parameters can be looked into, measured and hence the fluxes can be better quantified.

2.2.2. Open water interactions

The uptake or release of CO_2 by the open water in the Arctic is influenced by several factors. Physically, this exchange is estimated to be a function of wind speed, salinity, temperature and difference in partial pressure of CO_2 in the sea and the atmosphere (Fransson, Chierici et al. 2017). The main biological control is primary production which is sensitive to changes in the climate (Arrigo, van Dijken et al. 2008).

In a recent study, Yasunaka, Siswanto et al. (2018) estimated monthly air -sea CO_2 flux in the Arctic Ocean and regions above 60° N between 1997-2014. They used chlorophyll a, pCO_2, sea surface temperatures, sea ice salinity, sea ice concentration, atmospheric-mixing CO_2 ratio and the geographical location data to generate self-organizing maps of surface partial pressure of CO_2. They found the surface partial pressure of CO_2 and chlorophyll-a to be negatively correlated which is plausible as a high cholorophyll-a points at higher biological activity. In all the analysed regions, they also found a strong uptake in October when the wind speeds are high and the pCO_2 is still low. They estimated an annual uptake of 180 Tg C yr^{-1} of CO_2 with a large uncertainty of ± 130 Tg C yr^{-1}, establishing the need for more measurements and improved model calibrations. Globally, between 2000-2017, all oceans are estimated to have taken up to 2430 ± 670 Tg C yr^{-1} (CarbonTracker 2018). Therefore, according to the above estimates, approximately 7.4% of the total uptake can be attributed to the Arctic ocean, making it an important sink for global CO_2. An increase in the net rate of production has been already reported by Arrigo, van Dijken et al. (2008). They also

used satellite derived sea ice data, SST and chlorophyll data along with a primary production algorithm to estimate the annual primary production in the Arctic region. They found that the primary production increased by a yearly average of 27.5 Tg C yr^{-1} between 2003-2006 and 35 Tg C yr^{-1} between 2006 and 2007. They ascribed 30% of this increase in Arctic primary productivity to the decreased minimum summer ice extent and the remaining to the extended growth season of the phytoplankton. When taken into consideration with the total estimate of 180 Tg C yr^{-1} discussed above, these values indicate a ~16% increase over 3 years which signals towards the consequences of a warming Arctic climate.

2.2.3. Physical Processes

As mentioned in the introduction, sea ice was earlier believed to restrict gaseous exchange but it has been found to be permeable under certain conditions of temperature and salinity (Delille, Vancoppenolle et al. 2014, Kotovitch, Moreau et al. 2016). Gosink, Pearson et al. (1976) were one of the first to propose that unlike freshwater and lake ice, sea ice is permeable to gases when surface temperatures are above -15°C. Golden, Ackley et al. (1998) reported a theoretical threshold of a brine fraction above 5% and temperature above -5°C to be suitable for permeability of liquids within the sea ice which can be extended to gases as well (Delille, Vancoppenolle et al. 2014). Further, Zhou, Delille et al. (2013) reported that a salinity range of 7.5%-10% resulted in an enhanced bubbling of Argon from the sea ice and this could also be true for CO_2 (and CH_4).

Within the sea ice, gases can be found in the dissolved phase (in the brine channels) and in the form of bubbles. The latter are formed when a decrease in temperature during winter, causes the brine inclusions to shrink and which increases the concentrations of gases, such as CO_2, along with the salt (Kotovitch, Moreau et al. 2016). This in turn leads to formation of bubbles of the gases. These bubbles have been observed at the start of the ice formation and are suspected to continue forming during the growth of the ice. These bubbles may be released into the atmosphere if they are able to rise due to buoyancy. When the ice begins to melt, dilution of the brine results in dissolution of

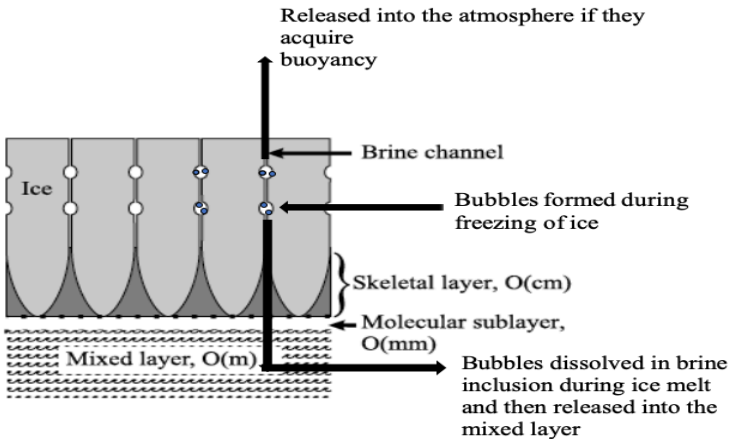

Figure 4 Schematic representation of CO_2 within sea ice. Adapted from "Modelling ice algal growth and decline in a seasonally ice-covered region of the Arctic (Resolute Passage, Canadian Archipelago)" by D. Lavoie, K. Denmann & C. Michel, 2005, Journal of Geophysical Research,110, C11009, pg 2, Adapted with permission.

the gas bubbles back into the brine inclusions (Kotovitch, Moreau et al. 2016). Subsequently, the salt and gases are released into the underlying water column through gravity drainage or flushing or convective mixing. This process is schematically represented in Figure 4. Over the years, our understanding of the above discussed processes has mainly been improved through lab experiments which simulate the formation and melt of sea-ice. These have helped to fill in the knowledge gap created due to lack of in-situ measurements (see Tison, Haas et al. (2002), Nomura, Yoshikawa-Inoue et al. (2006), Kotovitch, Moreau et al. (2016)). However, these experiments are often limited by the sample collection techniques and potentially impose stress to the organisms during the process. Hence, in-situ measurements are still needed to validate these results.

2.3. Link between DMS and CO_2

Several years of research on DMS and CO_2 has improved our understanding of the influence of the gases in the Arctic but it is still incomplete. As can be seen from above, increased area of open water can lead to enhanced CO_2 uptake. This in turn can further enhance the primary productivity of sea ice algae and phytoplankton, thereby signalling an increased DMS release. This may lead to enhanced CCN and hence have a compensating effect on the climate. However, this mechanism maybe limited by the acidification of ocean due to CO_2 uptake, nutrient availability, change in phytoplankton species etc. The needs of the modelling community in terms of algae and phytoplankton are further elaborated and highlighted in Steiner, Deal et al. (2016). Further, changes in the nature of sea ice, formation of melt ponds can also influence the CO_2 and DMS production.

Given all these uncertainties, there is a need for a comprehensive study such as MOSAiC to gather additional information about the inherent processes involved. This will enable us to make predictions of the future climate of the Arctic and consequently its influence on the entire planet's climate.

3. Methodology

In this section we elaborate the research methodology used in this thesis regarding the implementation and application of modelling experiments to further investigate the sea-ice/ocean/atmosphere processes and interactions involved in the Arctic DMS cycle (see Figure 5). In section 3.1,we explain the implementation of the Hayashida, Steiner et al. (2017) DMS model in a box-model setup. Next, the sea-to-air DMS fluxes simulated with this box modelling system served as input to a 1-D Single Column meteorological and atmospheric chemistry Model (SCM) to obtain DMS mixing ratios in the lower troposphere. This is explained in more detail in section 3.2. In order to validate the SCM results, observations obtained from a weather station at Resolute Airport were used to evaluate the model simulated meteorological drivers of DMS cycling and exchange, as elaborated upon in section 3.3.

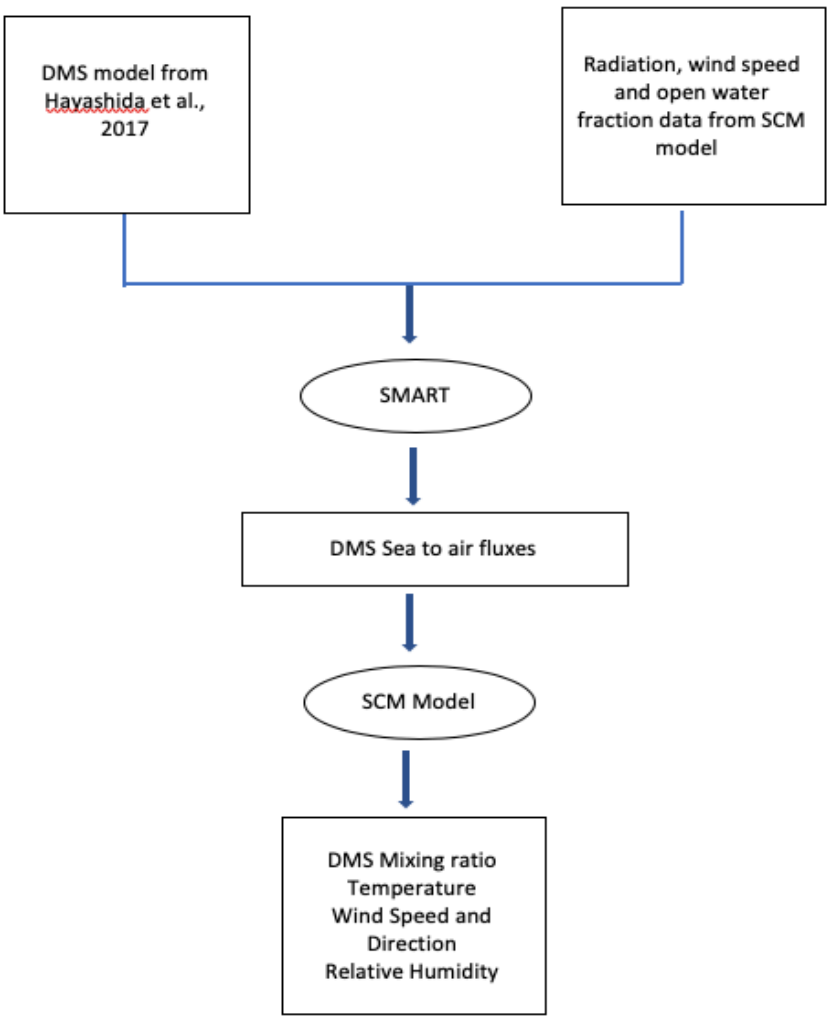

Figure 5 Flowchart depicting the methodology used in this thesis. The boxes represent the input and output data while the circles represent the models used.

3.1. SMART implementation

In this thesis, the box modelling software package Simulation and Modelling Assistant for Research and Training (SMART) (Kramer and Scholten 2001) was used to implement the 1-D DMS model developed by Hayashida, Steiner et al. (2017). They developed this model within the framework of an existing coupled sea-ice ocean ecosystem model designed by Mortenson, Hayashida et al. (2017)to estimate DMS fluxes. The model calculates the DMSP and DMS for both the sea-ice and underlying water column by using parameterizations and input from an ocean physical model developed by Flato and Brown (1996). Hayashida, Steiner et al. (2017) presented their modelling system providing a detailed description of the most salient features and then showing application of the model. They conducted simulations considering the seasonal changes in sea-ice dynamics of landfast first year-ice in Resolute passage, Nunavut, Canada (74º 42.6' N, 95º 15' W) between 1st February-1st July, 2010. They chose this location (see Figure 6) due to the availability of DMSPp and DMSPd measurements obtained during the Arctic Ice-Covered Ecosystem (Arctic-ICE) study in May-June 2010 to validate their results. The measurement site was about 10 km from the Resolute Bay airport and has a predominant North-western wind direction (Hudson, Aihoshi et al. 2001). For more details see Hayashida, Steiner et al. (2017).

SMART was chosen for this study due to its user-friendly and simple interface which allows the user to implement a dynamic modelling system described by a number of state variables. The temporal changes of these variables are determined by differential equations determined by the source and sink processes and, finally, applied constants using a box model approach. SMART was chosen instead of the more advanced Fortran system because the former allows for a thorough understanding of the underlying mechanisms in the box model set-up and is usable even by non-modellers, for example, MOSAiC experimentalists.

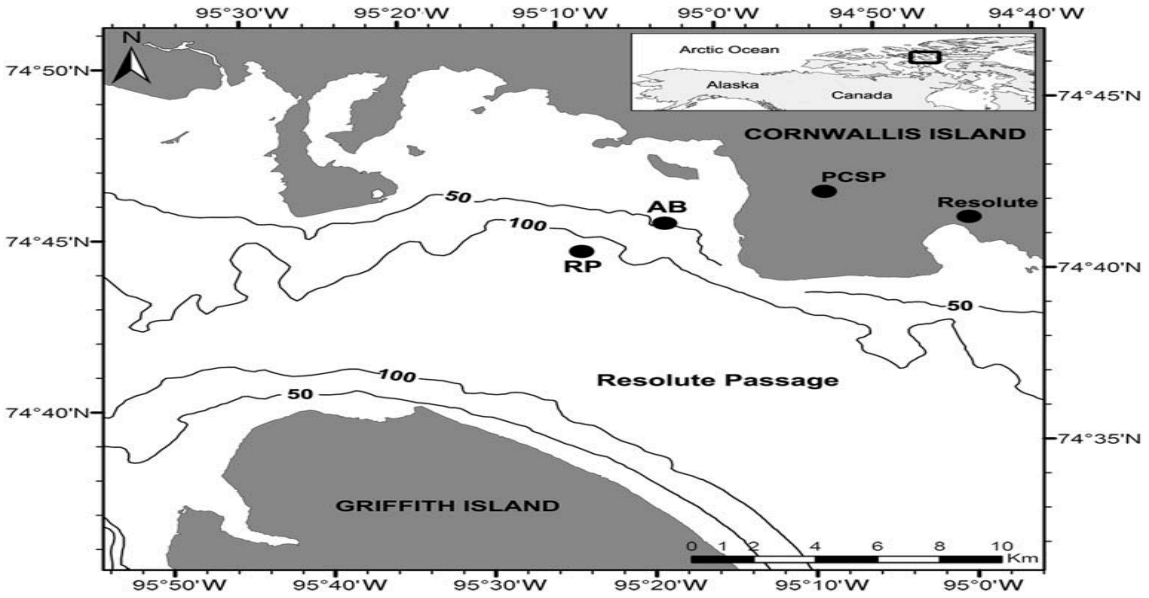

Figure 6 Location of Landfast ice at Resolute for Hayashida et al. 2017 runs (RP) and Resolute Bay Airport (Resolute). Reprinted from "Biological and physical processes influencing sea ice, under-ice algae, and dimethyl sulfoniopropionate during spring in the Canadian Arctic Archipelago" by V. Galindo et al., 2014, Journal of Geophysical Research Oceans, 119, pg 3748, Copyright 2014 by American Geophysical Union.

The SMART model was run for the same location but for a longer time period. In our case, the model was run from 1st February to 3rd September, 2010 (215 days) with an

integration step of 1 day in accordance with the model simulation presented in Hayashida, Steiner et al. (2017). We chose a longer time period when compared to them as it contains a part of the Arctic winter, the polar sunrise, early spring and Arctic summer (when the algal bloom is at its peak) and is well-suited to the long duration of the MOSAiC experiment. It was implemented in two steps, firstly focussing on implementation of the sea-ice module followed by the implementation and coupling to the underlying water column model. The chosen numerical integration scheme was Rkqs integration method, an advanced variant of the 4th order Runge-Kutta algorithm. In this method, the consecutive values of state variables and errors are calculated by a "balanced weighting scheme of intermediate derivatives" (Kramer and Scholten 2001). It was chosen because it is the most advanced scheme available in SMART and allows the system to resolve a simulation using a flexible timestep dependent on the time scale of changes in the state variables.

As the original model of Hayashida et al. (2017) is coupled in a Fortran environment along with a physical and ecosystem model, the SMART model had to be constrained with a selection of the physical and ecosystem drivers using the SMART option to read in a tabular data file to provide the model with input data.

In the SMART model, the concentrations of DMSPd and DMS in the bottom most layer of sea-ice, 0.3m, and the underlying water column were the state variables. The involved source and sink processes were implemented as auxiliary variables (see Table 1, Fig 3 in Chapter 2). Most constants and parameters used to define the processes were intuitively included in the constants and parameters section (see Appendix, Table 1). However, some variables that could not be parameterized using a formula were included in tabulated form. The data for these tabulated parameters was obtained from other studies within this region (see Appendix, Table 2). The tabulated data for radiation, wind speed and open water fraction data was obtained from SCM runs for this location. Note that pseudo-constants were not used in our model.

Table 1 The source and sink terms used to concentrations of DMSPd and DMS in sea ice and underlying water column in Hayashida et al., 2017 model

Region	State variable	Sources	Sinks
Sea ice	DMSPd	Cell lysis (Flysis), Exudation (Fexud)	Consumption (Fdmspdc), Free DMSP-lyase (Ffree) Release (Fdmspdr)
	DMS	Conversion by bacteria (Fconversion) Ffree	Consumption (Fdmsc) Photolysis (Fphotolysis), Release (Fdmsr)
Water column	DMSPdwc	Cell lysis (Fwclysis) Sloppy feeding (Fwcsloppy), Vertical diffusion of DMSPd (Fverticaldiff_DMSPdwc) Release from ice to water column (Fdmspdwics)	Consumption (Fwcdmspdc), Free lyase (Fwcfree)
	DMSwc	Conversion by bacteria (Fwcconversion) Fwcfree, Vertical diffusion of DMS (Fverticaldiff_DMSwc) Release from ice to water column (Fdmswcis)	Photolysis (Fwcphotolysis) Sea to air flux (Fseaair) Consumption (Fdmswcc)

The SMART simulated sea to air DMS fluxes served subsequently as input for the SCM to obtain the DMS mixing ratios for the same time period.

3.2. Single Column Model (SCM)

The SCM is a 1-D model that is used to perform detailed atmospheric chemistry studies with a focus on surface and boundary layer meteorological and chemistry interactions. This coupled 1-D chemistry-climate modelling system has been applied in many studies to analyse field scale observations (e.g. Ganzeveld, Eerdekens et al. (2008), Kuhn, Ganzeveld et al. (2010), Seok, Helmig et al. (2013). The SCM has also been applied to further develop and evaluate improved representations of surface exchange processes, e.g., a multi-layer canopy exchange modelling system (Ganzeveld, Lelieveld et al. 2002) for application in global chemistry and climate models (Ganzeveld, Lelieveld et al. 2002, Ganzeveld, Bouwman et al. 2010). In the SCM application, the surface exchange process simulations form an essential part of the coupling between global model representations of atmospheric chemistry (Roelofs, Lelieveld et al. 1998, Ganzeveld, Bouwman et al. 2010) and a representation of the ECHAM4 (**EC**MWF **HAM**burg) physics in a single column setup.

The SCM was used to carry out an online calculation of the meteorological and chemical dynamics within a vertical column for the location resembling the measurement site nearby Resolute. The model simulated online, starting from the initial vertical profiles of temperature, moisture and wind speed and prescribed surface properties (e.g. surface cover fraction, albedo, roughness, moisture content) and the temporal variability in meteorology and hydrology. The last term also largely drives the atmospheric chemistry processes such as natural emissions, deposition, oxidation chemistry and turbulent and convective transport processes. An important feature of the model is that it can be "nudged" using observed meteorological and atmospheric chemistry parameters also to consider the contribution by advection in such a 1-D model set-up. Nudging is defined as a form of data assimilation which allows us to obtain a realistic representation of the actually observed meteorological conditions using meteorological reanalysis data (n.d.). This nudging, using the difference between the ECMWF data and the simulated data can be interpreted as adding implicitly the "advection tendency" to complement all the other column processes being explicitly resolved in the model. In our case, the model is nudged using ECMWF reanalysis data regarding wind speed (u, v and w), temperature, moisture and liquid water content. The strength of the nudging is determined by a "relaxation co-efficient" which is recommended to be 1/ time interval between analysis results (in seconds) (n.d.). As ECMWF reanalysis data is obtained at 6 hourly intervals, in our case, the relaxation coefficient was 1/ 6 hours (21600 s). To also consider the long-term differences in the chemical boundary condition, we have also nudged the free tropospheric concentrations of the long-lived tracers O_3, carbon monoxide (CO), NO_x and SO_2 using the Copernicus Atmosphere Monitoring Service (CAMS) near-real-time dataset. (https://atmosphere.copernicus.eu/).

As mentioned above, the model was first used to obtain the input data regarding net radiation, wind speed for the SMART model simulations. Next, with the obtained DMS sea-to-air flux, the model was rerun to obtain DMS mixing ratio values for the same period. The SCM's simulated meteorological parameters have been validated with measurements obtained at the weather station at Resolute Airport as described in the section below.

3.3. Model validation

It is standard practice to evaluate a model's meteorological performance along with the atmospheric chemistry also given the important role of many meteorological (and hydrological) drivers of atmospheric chemistry source and sink processes. Here, we validate the SCM results using data obtained from measurements at Resolute Airport, located 7km away from the Hayashida, Steiner et al. (2017) site (see Fig 7). Hourly observation data for the entire time period was obtained from The Government of Canada's historic weather database. The variables included in this validation were wind speed, direction, temperature and relative humidity.

Resolute Bay Airport is located on a peninsula at the southern tip of the Cornwallis Island, Nunavut, Canada (74º 72' N, 94º 97' W). The elevation is ~67 m ASL. The WMO ID of that station is 71924. The terrain is gently rolling in nature and slopes down to the south and west, toward the sea. To the northeast, ~0.8 km away, there are about 400m high hills which rise to an upland plateau with rolling slopes. Also, 5 km south-southwest to the station lies Cape Martyr (~174 m) and about 3 km east-south east lies Signal Hill (~192 m). These orographic features around the airport could have an influence on the meteorological measurements, especially regarding wind speed and direction.

The simulated data was statistically validated by calculating the regression co-efficient (R^2), Mean Bias Error (MBE) and Root Mean Square Error (RMSE). These gave us an insight of the model's performance when compared to the observations obtained from the Resolute Airport.

4. Results

4.1. SMART model results

The SMART model was used to obtain the concentrations of DMSPd and DMS in the water column and sea ice. The sea to air flux was also obtained from the model and was subsequently used as input for the SCM to simulate the resulting atmospheric DMS concentrations and cycling. In the section below, the obtained results are presented and we also discuss the model's performance compared to the modelling results from Hayashida, Steiner et al. (2017) (hereafter referred to as HY2017).

4.1.1. DMSPd concentrations

Figure 7 shows the simulated DMSPd concentrations in the bottom ice and the under-ice water column for the Resolute case study from February until end of August. In the bottom ice, the DMSPd concentration begins to rise in early spring, mid-March and April reaching concentrations of 600 nmol L^{-1}. The peak value of ~1800 nmol L^{-1} is reached at the beginning of June, comparable to the model simulations of HY2017. The main difference between the SMART simulations and their model results is that the SMART model simulation shows some relative short-term changes. For e.g., a sudden decrease in the bottom ice DMSPd mid-April and a short pause in its decrease end of June, when compared to the HY2017's results which generally show an overall smoother temporal variability. This is not what we expected as the SMART model is constrained with prescribed constant parameters regarding the biogeochemical conditions, e.g., nutrient availability, ice algal growth whereas HY2017 used a model setup in which these parameters are provided by the coupled ecosystem and ocean physical model. However, when we looked into the underlying source and sink terms, we found that these differences can also be explained by how we prescribed parameters. For example, the sudden drop observed in April can be explained by the drop in the prescribed nutrition limitation index value at the same moment (Mortenson, Hayashida et al. 2017, p8) which in turn affects the source of DMSPd associated exudation and the sink of DMSPd due to consumption. It indicates that a better representation of the nutrient limitation in SMART could make our results more comparable.

The simulated under-ice DMSPd concentrations are overestimated in the SMART model compared to the results of HY2017. In their study the initial concentrations are close to zero before they peak (~6.25 nmol L^{-1}) while in the SMART model the DMSPd concentrations rise to ~2 nmol L^{-1} and stay constant until the simulated strong increase in late spring reaching a peak value of ~9 nmol L^{-1}. This difference is primarily due to a fixed rate of sloppy feeding in the SMART model. In order to calculate the rate of sloppy feeding we used fixed value for loss rates of small and large phytoplankton due to grazing by zooplankton (Rp1z1 and R2p2z2, see Appendix, Table 1) in the SMART model due to lack of observational data for grazing rates in the Arctic (Hayashida, Steiner et al. 2017). In HY2017, it is calculated by the ocean ecosystem module. Hence, this source term has a constant value in our model throughout the simulation while in HY2017, it only becomes significant in the month of June (Figure 4b in HY2017). We tested this by eliminating sloppy feeding term in a simulation and the initial overestimation reduced from ~2 nmol L^{-1} to ~0.2 nmol L^{-1}. Hence, there is a need to

collect data on zooplankton grazing rates in the Arctic to improve these Arctic DMS cycle model simulations.

Despite of the difference in the simulated peak values in SMART and HY2017, an average site peak value of 11 nmol L^{-1} was reported from the observations from the Arctic – ICE campaign (Hayashida, Steiner et al. 2017). This indicates that our result is not entirely unrealistic. The simulated peak is also obtained with a lag of a few days compared to the simulations by HY2017. It is simulated in the beginning of July rather end of June, which could be due to the difference in initializations of the two models.

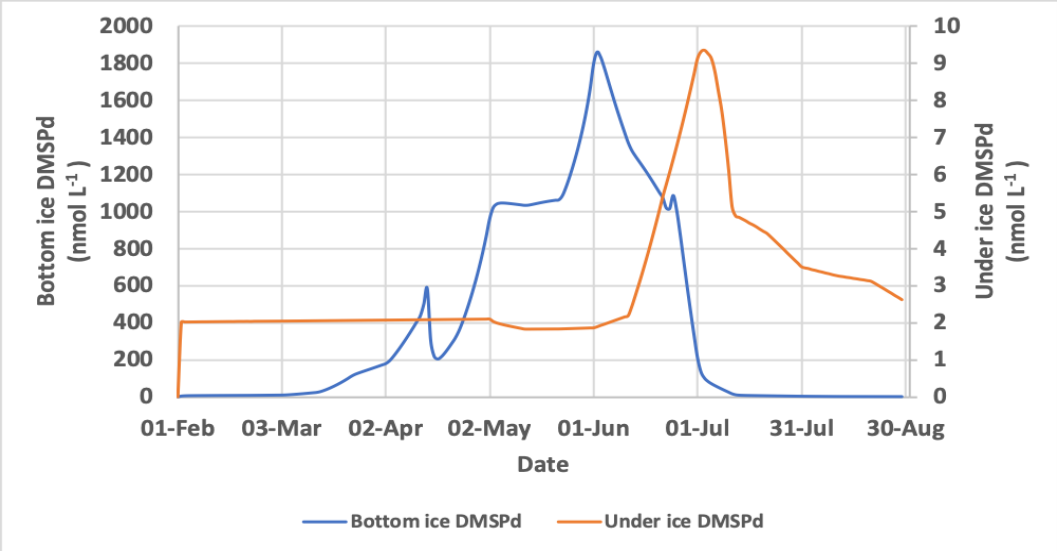

Figure 7 Time series of simulated DMSPd concentrations (nmol L^{-1}) in the bottom ice (blue line) and under ice water (orange line) between 1 February- 1 September, 2010.

4.1.2. DMS concentrations

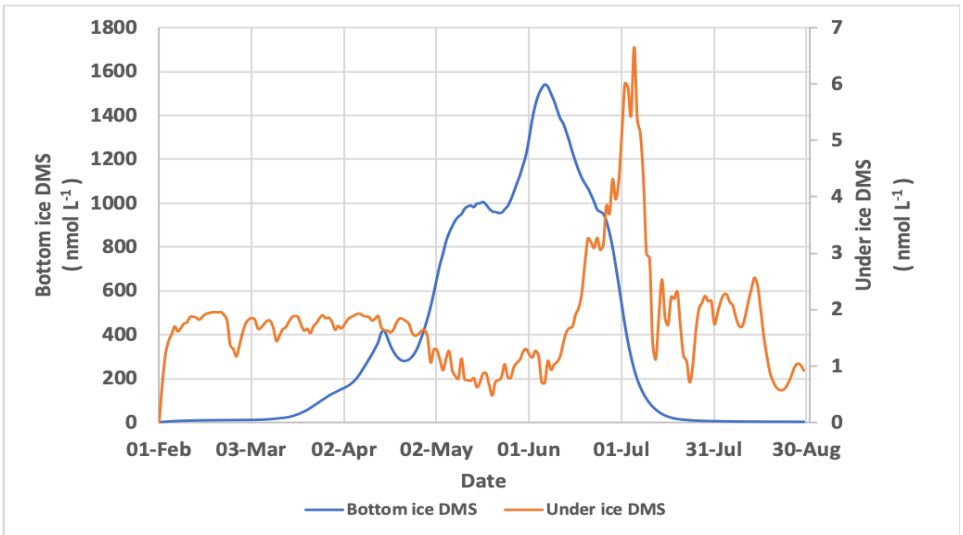

Figure 8 Time series of simulated DMS concentrations (nmol L-1) in the bottom ice (blue line) and under ice water (orange line) between 1 February- 1 September, 2010.

The bottom ice DMS concentrations are well simulated when compared to HY2017 (Figure 10). The simulated initial concentrations and the increase in production are well reproduced by the SMART model. The peak value of ~1600 nmol L^{-1} and its occurrence, in the beginning of June, is in agreement with the results of HY2017. These values are also comparable to measured values of 2000 nmol L^{-1}, reported by Levasseur (2013). This indicates that our SMART model implementation is able to simulate well the source and sink term for this variable. However, here again we see some differences such as the drop in April, which can be explained by the same reasons as discussed for DMSPd in the sea ice. This is because the source term of bacterial conversion of DMSPd into DMS depends on the rate of consumption of DMSP. The rate of consumption, in turn, depends on the value of the nutrient limitation index. These interlinkages and dependencies demonstrate the need for accurate and robust measurement of the source and sink processes.

The initial concentrations of under-ice DMS concentrations are overestimated by the SMART model, which can also be explained by the fixed sloppy feeding rate as discussed above for DMSPd in the water column. This is because, as discussed above, the source term for bacterial conversion depends on the DMSPdwc concentration, which is influenced by the rate of sloppy feeding. The simulated peak of ~6.5 nmol L^{-1} is obtained with a lag of about a week and is slightly lower than that simulated by HY2017 of ~9 nmol L^{-1}. However, this can also be explained by the fact that in their modelling analysis they have not considered the DMS sea to air flux resulting in higher DMS concentrations in the water. The delay can be explained due to the lag also seen in the under ice DMSPd production.

The SMART model simulated sea to air flux is also comparable to the findings of HY2017. Here it is interesting to note the much higher temporal variability in the DMS emission flux compared to the temporal variability in DMS concentrations. This higher variability in the flux is also associated with the high variability in wind speed as it is one of the main drivers of DMS ocean-atmosphere exchange fluxes besides oceanic DMS concentrations. HY2017 carried out experiments assuming four different open water fractions and reported a maximum flux of 8.1 µmol m^{-2} d^{-1} for an open water fraction of 1.0. The SMART simulations show a gradual rise in DMS release and the highest flux of 3.8 µmol m^{-2} d^{-1} in the first week of July. The algal bloom is then at its peak and the sea ice cover is simulated to be at a minimum by the SCM. The differences between the peak values can be explained by the above discussed parameterizations, fixed values and interlinkages between processes that ultimately determine the sea to air flux. Furthermore, there can be significant influence of meteorological conditions of temperature and wind. These meteorological conditions and the implications of this flux for DMS concentrations in the atmosphere are discussed in the following section.

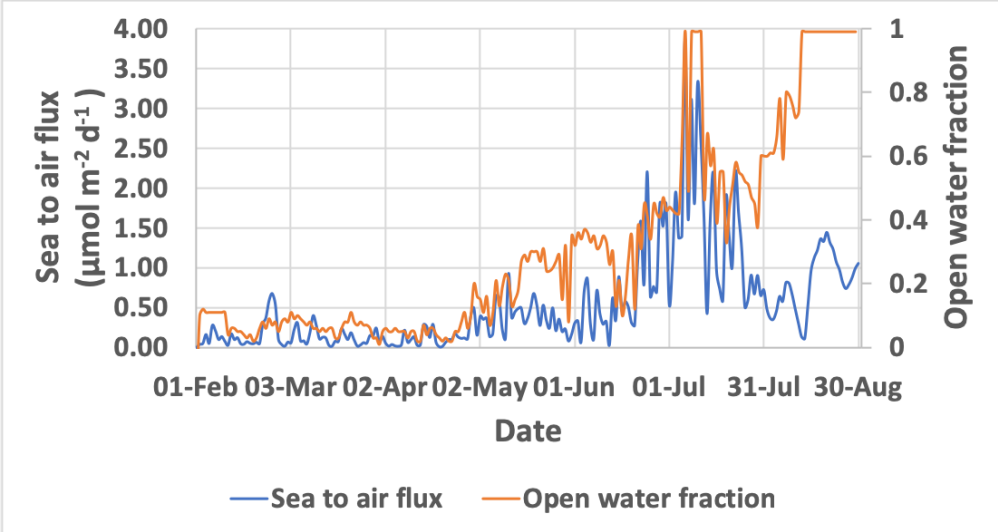

Figure 9 Simulated sea to air DMS flux plotted along with open water fraction between 1 February- 1 September, 2010

4.2. Single Column Model (SCM)

In this section, we present the results obtained from the simulations with the SCM. The simulated micrometeorology was evaluated using measurements from Resolute Airport Weather Station located 10 km away from the field site also described in the methodology. We first consider the entire time period of the model run. Subsequently, we focus on June and July, the bloom period of the phytoplankton.

The evaluated micrometeorological data includes – wind speed, wind direction, temperature, boundary layer depth and relative humidity. Further, the simulated temporal variability in DMS mixing ratio is presented to also evaluate how the simulated DMS fluxes reflect in atmospheric DMS mixing ratios as a function of these emissions, mixing conditions and chemistry.

4.2.1. Full time period

The SCM simulated wind speed is consistently underestimated by the model over the entire time period (see Figure 12). While the overall behaviour in terms of temporal changes is comparable, the model does not capture the extremes. This is also reflected in the results of the statistical analysis as seen in Table 1. This underestimation could lead to a too shallow boundary layer with little mixing in the model when compared to observations. It is noteworthy to remember that the distance and difference in orography between the two locations could explain some of the differences between the SCM simulated and observed wind speed. Another possible explanation could be the selected value of the relaxation coefficient used to the nudge the model towards the ECMWF data. However, our analysis showed that the ECMWF wind speed, used to nudge the SCM simulated wind speed, was comparable to the SCM results. This implies that enhancing the relaxation coefficient to more strongly nudge the SCM model towards the ECMWF would not result in better simulations. It indicates that this discrepancy regarding the simulated and observed wind speed is mainly due to the representativeness of the ~20 km resolution ECMWF wind speed for the grid box resembling the measurement location.

Table 2 Summary of statistical parameters used to compare results from SCM against the measured data

Parameter	Statistical metric		
	R^2	RMSE	MBE
Wind	0.071	3.97	-1.79
Temperature	0.89	4.82	0.85
Relative humidity	0.09	0.18	0.18

As seen in Figure 13, the estimated model air temperature, at 10m height, generally, agrees well with the observed air temperature (see Table 1). In the beginning of the run, the model shows slightly warmer temperatures compared to the observations but during the bloom period (June-July), the model shows lower temperatures. An important consideration here is the method used by the 1-D model to calculate surface temperatures. The SCM calculates the surface temperature considering the sea ice fraction, the prescribed SST and the explicitly calculated (sea-ice) skin temperature. This SST resembles the ECMWF SST for this particular location. Consequently, most likely an underestimation of the surface (and air) temperatures by the ECMWF for this location, combined with an opening ocean with the decrease in sea-ice extent in late spring and summer explains, to a large extent, the model underestimation of temperature.

The model overestimates the humidity, especially in the months of February-March and June- July, the bloom period (see Appendix, Figure 1). This is also reflected in the low R^2 value and MBE comparing the SCM simulated and observed relative humidity as shown in Table 1. Note that a small difference in the absolute humidity along with the low winter temperatures could result in large errors in the relative humidity calculation. In winter, when the observed absolute humidity is small (see Appendix, Figure 2), and the SCM simulated temperatures are slightly higher than the observed, the relative humidity is overestimated. During the bloom period, the absolute humidity is comparatively higher, however, the model simulated air temperature is lower compared to the observations. This results in a simulated occurrence of a very stable conditions with the presence of a strong inversion present and consequently, the simulated relative humidity is higher than the observed.

The SCM simulated boundary layer (BL) height is shown along with DMS mixing ratio values in Figure 14. First, focusing on the simulated BL height, it is interesting to see that the winter and early spring has a higher BL height compared to the summer, a response quite opposite to what is generally observed for continental sites. Due to lack of observational data from the campaign, these simulated BL heights were compared to output from a (present-day climate) simulation with global climate-chemistry modelling system EMAC (Ganzeveld, Bouwman et al. 2010). This showed us that in February-March and during June and July, the 1-D model simulates a BL height that is substantially smaller compared to that of the global modelling system. Around May, the opposite is true. However, this overall long-term trend of a simulated decrease in the BL height from winter/early spring into the summer is also observed in the EMAC simulations. It coincides with the end of the frozen season in the Arctic (Hudson, Aihoshi et al. 2001). Some of the SCM simulated very shallow BL heights can be explained by the underestimation of temperatures (only during bloom) but also potentially by an underestimation of wind speed in the SCM (and ECMWF) during these periods.

Figure 12 shows that the simulated DMS concentrations are very low in winter and early spring followed by a strong increase up to 3.5 ppbv during the peak algal bloom during summer. This is discussed in more detail in the section below.

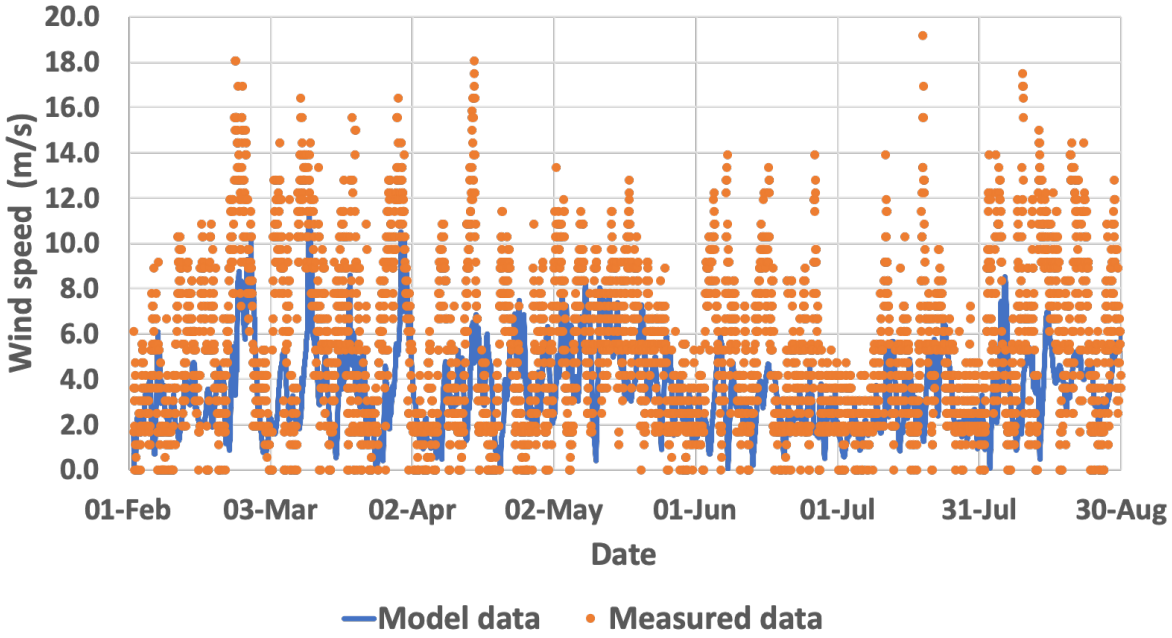

Figure 10 Simulated wind speed from SCM (blue) and measured at Resolute Airport (orange dots) between 1 February- 1 September, 2010.

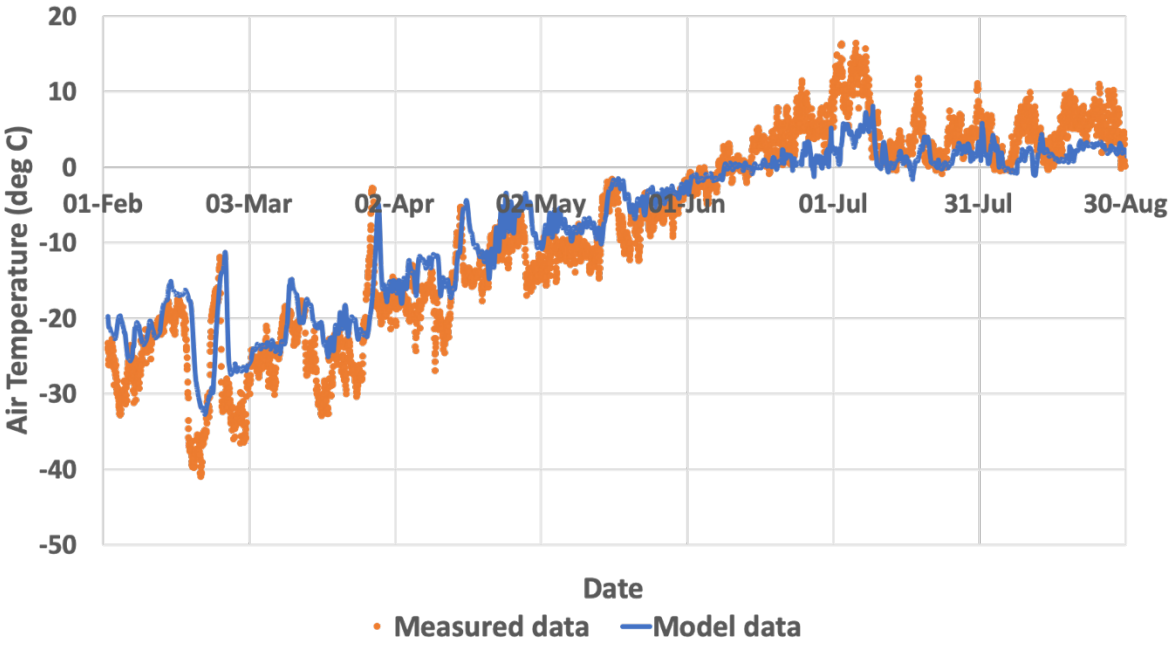

Figure 11 Simulated air temperature from SCM (blue) and measured at Resolute Airport (orange dots) between 1 February- 1 September, 2010.

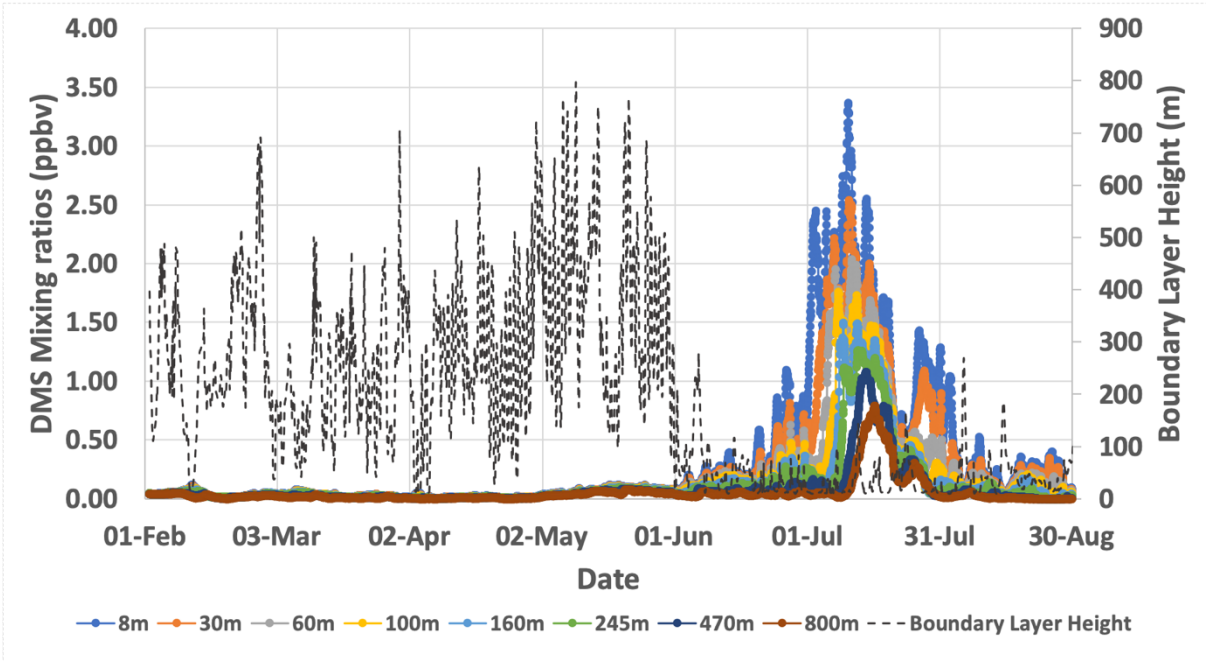

Figure 12 Simulated DMS mixing ratios from SCM up to 800m height with superimposed boundary layer height for the same time period (dashed line) between 1 February- 1 September, 2010.

4.2.2. Bloom Period (June-July)

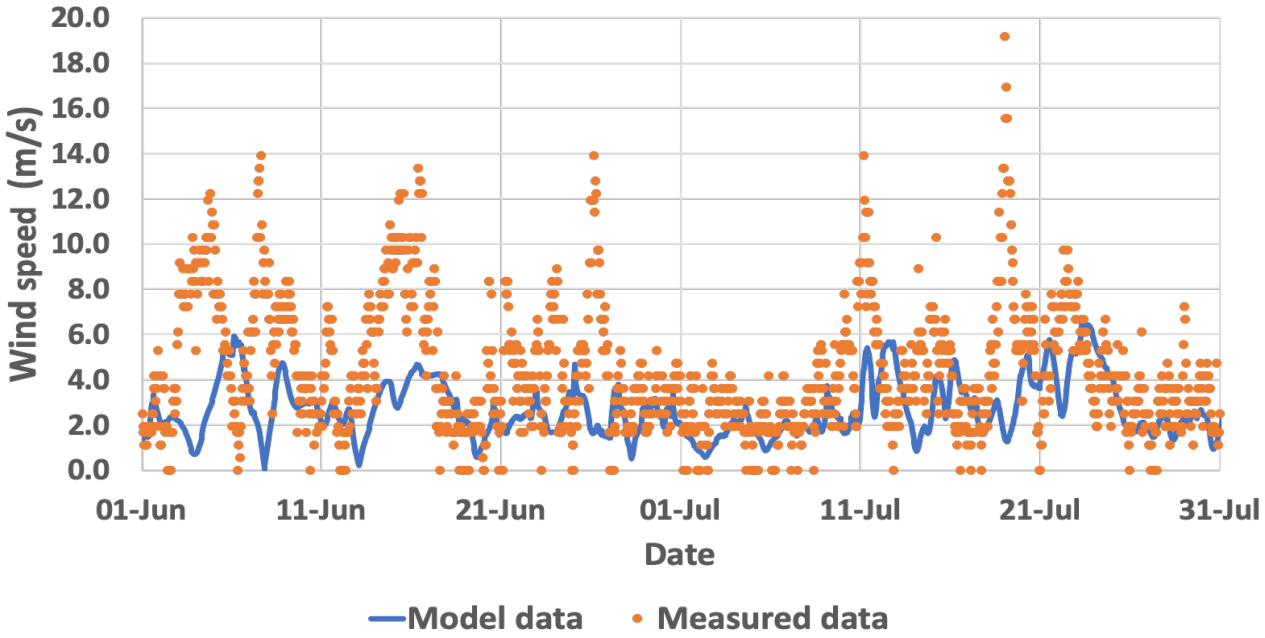

Figure 13 Simulated wind speed from SCM (blue) and measured at Resolute Airport (orange dots) from 1 June-31 July,2010.

As mentioned above, the model underestimates the wind speeds over most of the bloom period (see Figure 13). Nevertheless, between 1-11 July, 2010 when we see the largest simulated DMS concentration, the difference between simulated and measured wind speeds is comparatively smaller than other days. The wind direction during this peak bloom is north-western, which is the prevalent wind direction in this region during this season (Aliabadi,

Staebler et al. 2015). In such wind direction conditions, there is generally also the transport of low clouds into the Resolute passage (Hudson, Aihoshi et al. 2001). This could have implications for BL mixing and the radiation balance of this Arctic location.

When we compare the SCM simulated and observed air temperature focussing on the bloom period, shown in Figure 14, it is clearly visible that the SCM underestimates the air temperature, especially during the 1-11 July, 2010 period. This is supported by temperature measurement data from a meteorological station set up during the Arctic-ICE field campaign in 2010 (Mundy, Gosselin et al. 2014). This discrepancy is expected to be mainly due to misrepresentation of ECMWF's SST for this location being applied to constrain the SCM as explained above. This must be further corroborated by in depth analysis of the ECMWF SST data as well as the SCM simulated energy balance. However, this beyond the scope of this study.

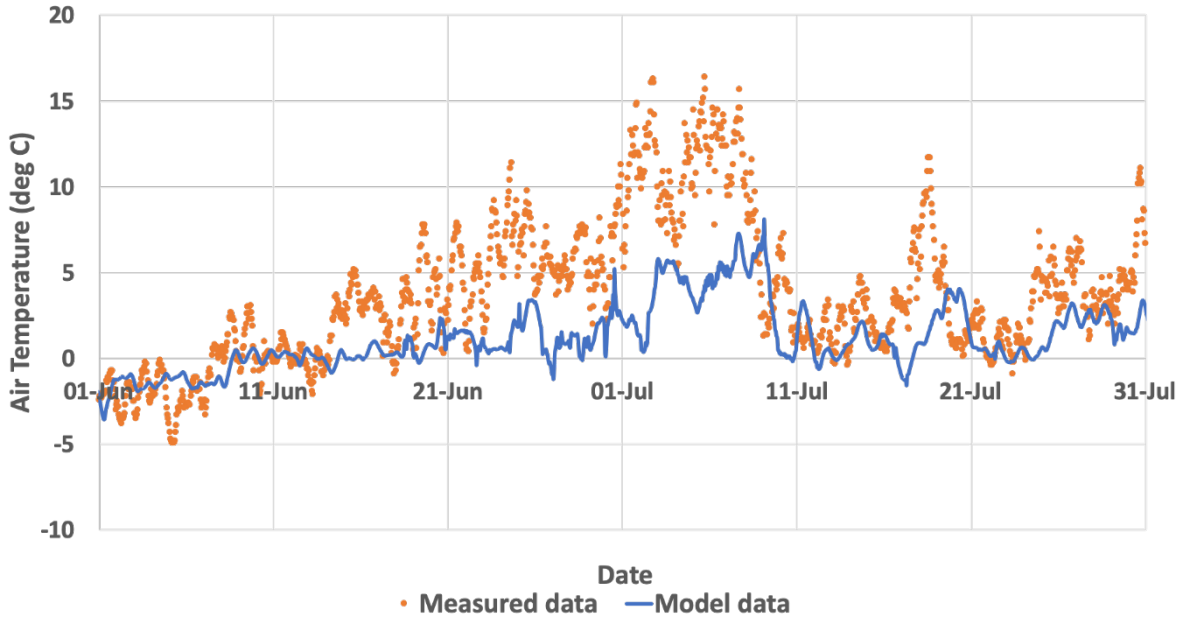

Figure 14 Simulated air temperature by SCM (blue) and measured at Resolute Airport (orange dots) from 1 June - 31 July, 2010.

Relative humidity (see Appendix, Figure 3) is again highly overestimated by the model. As discussed above, this overestimation can be partly attributed to the underestimation of the air temperature by the model. However, it also very likely that for the simulated very shallow BL heights, the increase in evaporation from the opening ocean could also result in this overestimation of the simulated relative humidity. Relative humidity has been found to play a major role on cloud properties in the Arctic (Cox, Walden et al. 2015), which stresses that the representation of such micrometeorological features should be carefully evaluated in such studies with a focus on the role of DMS in the Arctic.

The simulated BL is extremely shallow during the bloom period, indicating that the emitted DMS stays close to the surface and there is strongly supressed mixing (see Figure 16). This is further supported by the high value of the Richardson number, during the bloom periods. An underestimation of wind speed and misrepresentation of the temperature is most likely the main cause for the simulated very shallow BL height.

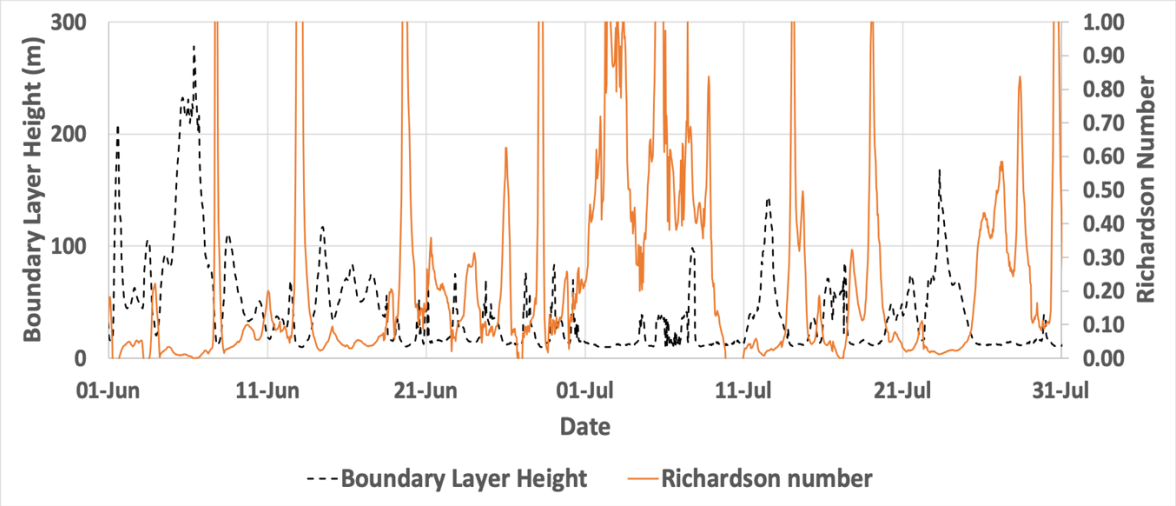

Figure 15 Boundary layer height (dashed lines) and Richardson number (orange line) from SCM model for 1 June-31 July, 2010

To evaluate the simulated DMS mixing ratios we rely on reported values from other campaigns since, unfortunately, atmospheric DMS was not measured during the Arctic-ICE campaign. DMS concentrations found in April and May by Park, Lee et al. (2018) were up to 0.45 ppbv of DMS at a measurement station (~474m) in Zeppelin mountain, Svalbard in 2015. Such spring time concentrations could be due to long range transport from the southern, open oceans (Abbatt, Leaitch et al. 2018). Between September and April, they found mixing ratios to be below the 0.0015 ppbv detection limit, which is also comparable to our simulations for February and March. Further, as expected, and shown in Figure 16, the highest DMS mixing ratios are seen in the layers closest to the surface. The simulated maximum DMS mixing ratio of 3-4 ppbv is significantly higher compared to other studies. For example, mixing ratios of up to 1.1 ppbv in July and August, 2014 (Mungall, Croft et al. 2016) and 1.8 ppbv in 2016 (Abbatt, Leaitch et al. 2018) have been reported from other Arctic locations. Similar high DMS mixing ratios have been reported for global model simulations for Amsterdam Island, a remote location in the Indian Ocean (Kloster, Feichter et al. 2006) however, for sea-ice free conditions.

Besides the lack of observations for these conditions, where all of the components of atmospheric DMS sources and cycling can jointly explain the occurrence of such high mixing ratios, it is also important to especially consider potential issues involved in the representation of the boundary layer in the model. The median BL heights in the Arctic for June and July have been found to be 430m and 180m, respectively (Cheng-Ying, Zhi-Qiu et al. 2011). Further, inversion base heights ranging between 100-300 m have been reported from various Arctic campaigns (Tjernstrom, Birch et al. 2012). Hence, given that SCM's surface layer is about 20m deep, an increase in the depth of the simulated inversion/mixed layer to about 150m would potentially reduce the concentration of DMS by about a factor of 7. For a diagnostically calculated inversion layer depth below this 20m there is no exchange between the surface layer and the overlaying atmosphere. This means that that all the emitted DMS is trapped in this 20m deep surface layer. Therefore, an improved estimation of the boundary layer could make our results more comparable. Furthermore, in this evaluation of the realism of DMS mixing ratios as high as 3 ppbv, we need to evaluate the role of chemical destruction of DMS into its oxidized products. As elaborated upon in the literature review, DMS may be actively oxidized to MSA, DMSO and SO_4^{2-} mainly through oxidation by OH radical and photolysis due to the 24-hour sunlight duration. These

products may further act as precursors to aerosol and CCN and in turn, impact the boundary layer height, radiation balance.

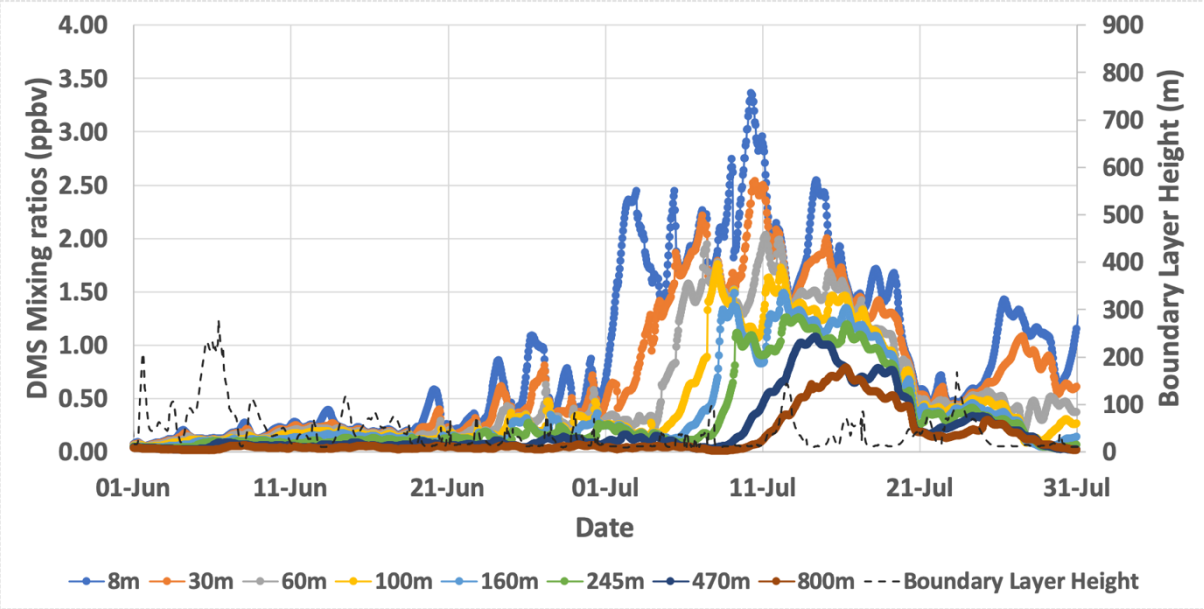

Figure 16 DMS mixing ratios obtained from SCM model up to 800m height with superimposed boundary layer height (dashed line) from 1 June - 31 July, 2010.

4.2.3. Sensitivity Analysis

To understand the role of boundary layer depth further, we carried out a sensitivity analysis in which we set the value of the Richardson number used in the stability correction functions for the surface exchange of heat and tracers (and not for momentum) to zero. We hypothesized that simulating such neutral boundary layer conditions would enhance the boundary layer depth and improve the simulated DMS mixing ratios.

The results were in contrast to our hypothesis. The boundary layer depth was only slightly altered and the DMS mixing ratios actually reached up to 10 ppbv around 8-9th of July as seen in Figure 17. Since, DMS mixing ratio values are also affected by atmospheric chemistry, we looked into the O_3 and OH radical concentrations simulated for the same time span. As seen in Figure 19, the modified representation of tracer exchange for stable conditions resulted in a simulated O_3 mixing ratio close to zero (see Appendix, Figure 4) whereas the minimum O_3 concentrations in the reference run ranged between 5-12 ppbv. This, further, resulted in low simulated OH concentrations (>0.5 10^{-6} molecules cm^{-3}, see Appendix, Figure 5), indicating that the oxidation of DMS is suppressed leading to higher concentrations compared to the reference simulation. It appears that the overall impact of this assumed modified representation of heat and tracer exchange for stable conditions results in a simulated change in the SCM's meteorological conditions such that the entrainment of O_3 into the surface layer from aloft is reduced. Note that these simulated O_3 concentrations are comparable to previous estimates of 0-40 ppbv in this region during this season (Anderson, Gregory et al. 1994). However, the representativeness of these values as well as the involved mechanism of the reduced oxidation concentrations in this simulation must be further evaluated to draw any concrete conclusions.

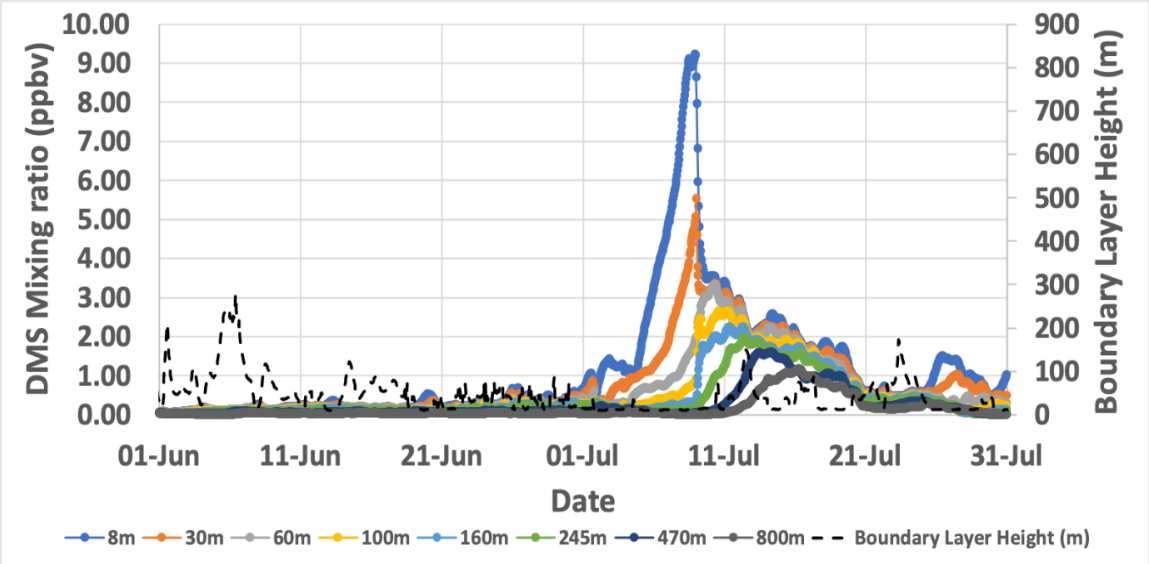

Figure 17 DMS mixing ratios obtained from SCM model up to 800m height with superimposed boundary layer height (dashed line) from 1 June - 31 July, 2010.

5. Discussion

One of the main objectives of this study was to identify the processes that are relevant for the production and exchange of DMS and CO_2 in the Arctic sea-ice, ocean and atmosphere. This was done by conducting a literature review and implementing a 1-D model representing the ocean – sea ice DMS cycling in SMART and using the simulated DMS fluxes in the SCM to simulate the resulting seasonal DMS concentrations as a function of these emissions, BL mixing and chemistry

The literature review stressed that biological processes involved in the production of DMS within the sea ice and underlying water column are of crucial importance for its release into the atmosphere. The precursor of DMS in the sea ice/water column is DMSP which is found in particulate form within the algal /phytoplankton cells and dissolved form in the water. The dissolved DMSP is converted to DMS by the action of free-lyase enzyme and fractional conversion of consumed DMSPd by bacteria. The main sinks of DMS are bacterial consumption, photolysis and loss to atmosphere. DMS in the atmosphere is oxidized into DMSO, MSA and SO_4^{2-} particles. The SO_4^{2-} particles contribute to the growth of CCN particles affecting cloud formation and radiation introducing a potentially relevant negative feedback on the climate as proposed by the CLAW hypothesis. However, no conclusive proof has been found for this theory (Vihma, Screen et al. 2016, Abbatt, Leaitch et al. 2018, Mahmood, von Salzen et al. 2018). Further, data is lacking on processes such as zooplankton grazing rates, the activity of the DMSP lyase enzyme, reduction of DMSO to DMS and the impact of the climate change on DMS production and the consequences for CCN in the atmosphere. Moreover, the multiphase chemistry of DMS oxidation (Hoffmann, Tilgner et al. 2016), halogen chemistry (Breider, Chipperfield et al. 2010) also need to be better measured and considered in future modelling studies (Steiner, Deal et al. 2016). The long-term (annual) observations of the MOSAiC project, including detailed biogeochemistry, meteorology and atmospheric chemistry observations complemented with modelling analysis as presented in this study, should help to improve our understanding of role of DMS and the aerosol feedback mechanism in the Arctic. It is important to note here, that this study is an attempt to consolidate all the essential information on DMS production and exchange in the Arctic. The review may not be complete due to time constraints and should be used as a starting step to understand the DMS cycle in the Arctic.

For CO_2, primary production in the sea ice and underlying water column form the largest sink for atmospheric CO_2 in the Arctic, especially during the summer months. In the winter, the Arctic sea-ice acts as a source of CO_2 through diffusion and gas-bubble formation. However, gas bubble formation has only been observed only in laboratory experiments (Kotovitch, Moreau et al. 2016). As for the consequences of the anticipated future warming, it is suspected that a more open Arctic ocean may take up more CO_2 from the atmosphere but the magnitude and duration of this is not known. It is important to measure and take into consideration several factors such as algal/phytoplankton species, nutrient availability, $CaCO_3$ precipitation etc., to draw conclusions about the role of the Arctic CO_2 cycle in future climate change (Arrigo, van Dijken et al. 2008, Steiner, Deal et al. 2016). Physical processes such as brine convection, bubbling through sea ice may also play an important role in CO_2 cycling and should be further evaluated. Lastly, it should be noted that in this study we limited the review to Arctic ocean - sea ice - atmosphere exchange. The role of CO_2 in the Arctic atmosphere and climate change have not been included in the review. There is extensive data is available on this topic including the link with changes in permafrost and tundra ecosystems dynamics but, this is beyond the scope of this study. However, it is important to consider in future studies, like the MOSAiC

experimental and modelling activities, the role of ocean- sea ice –atmosphere exchange relative to the overall changes in the Arctic sources /sinks and cycling of CO_2 at different temporal and spatial scales.

In order to enhance the understanding of the role of ocean- sea ice –atmosphere DMS cycling in Arctic climate, the Hayashida, Steiner et al. (2017) DMS model was implemented in the box modelling and simulation software program SMART. The overall simulated temporal variability and peak values that we obtained with this model implementation compared well with those of the HY2017. The original model was developed in Fortran and coupled along with a physical and ecosystem model. While the advanced Fortran code has an advantage that it is already coupled to an explicit representation of oceanic ecosystem- and physical processes driving the DMS cycling in the sea ice and oceanic surface layer, it can be a challenge to implement, especially for non-modellers, e.g. experimentalists. In contrast, the SMART model is a simple tool that only requires basic computing skills. It can be used for preliminary analysis of large datasets by non-experts and students, who are not skilled in programming or may not have a complete understanding of DMS cycling. Further, when constrained with relevant variables representative for other regions like Antarctica, with an anticipated different biogeochemical regime and available multiple-year of observations (J. Stefels, personal communications, 2018) the model performance can be further evaluated. Hence, the implementation in SMART opens the opportunity to enhance further studies focussing on DMS cycling by new researchers for other biogeochemical regimes.

Despite its applicability, the SMART model has its limitations. For example, some of the temporal dynamics in the SMART model results were different compared to the results by Hayashida, Steiner et al. (2017) although the SMART model reproduced well the overall behaviour in terms of magnitude of the DMS/DMSP concentrations and fluxes. These differences between our implementation and the modelling system can be due to different reasons. Firstly, the SMART model is constrained with some simple prescribed (constant) parameter values. For example, parameters like the sea ice thickness, sea ice fraction, ice algae biomass, nutrient availability etc., have to be prescribed due to lack of coupling with a physical and ecosystem model. Also, the release of DMSPd and DMS from sea ice to the underlying water column, is implemented using simple parameterizations when compared to Hayashida, Steiner et al. (2017) due to lack of explicit coupling to a physical model in our SMART implementation. Further, biological processes such as the phytoplankton growth rate, zooplankton grazing rates are fixed with constant values due to unavailable data and lack of coupling to an ecosystem model, respectively. Secondly, there are also inherent uncertainties in the rate constant values used for the model due to limited availability of measured value from campaigns (Steiner, Deal et al. 2016, Stefels, van Leeuwe et al. 2018) highlighting the need for campaigns like MOSAiC to better quantify these processes. Lastly, as already mentioned in Hayashida, Steiner et al. (2017), biogeochemical processes such as grazing of zooplankton on ice algae, activity of DMSP lyase enzyme, and reduction of DMSO into DMS in the sea ice and physical processes such as brine convection (see Figure 10 (pg 3145), Hayashida, Steiner et al. (2017)) have not been included in their model and hence also not in the SMART model.

Overall, we see that the SMART model is able to reproduce the Hayashida, Steiner et al. (2017) results well but is limited by the parameterizations and the application of some prescribed fixed or inferred varying input parameters. However, it has been proven to be a useful tool to enhance the understanding of DMS cycling by (other) non-experts and DMS cycling experimentalists also for other regions like Antarctica.

The results from the SCM model regarding simulation of a selection of micro-meteorological parameters indicate that the SCM seems to capture the longer-term (seasonal) changes well but there are some substantial differences between the observed and simulated values during some particular events. For example, in the bloom periods, the simulated air temperature and wind speed are underestimated whereas the relative humidity is overestimated. The misrepresentations of these parameters could be associated with a simulated very shallow boundary layer height during the bloom period and which also explains the simulated high DMS mixing ratios. It is important to remember here that the SCM model is nudged using ECMWF data including atmospheric temperature, moisture and wind speed as well as the sea ice fraction and SST. These data are representative for a grid resolution of ~20 km. It is possible that, at this resolution, ECMWF is unable to capture a local warming, for example of shallower coastal zone compared to the representation of the oceanic surface layer in the ECMWF system, resulting in an underestimation of surface temperature which might result in an underestimated BL depth and too high moisture levels. The representativeness of ECMWF data for this location should be further evaluated before drawing further conclusions. Furthermore, the ~10km distance between the site of the DMS cycling observations and the meteorological measurement site (airport) should be considered as well. For example, the simulated relative humidity is overestimated when compared to the observations during the bloom period. This could be explained due to the presence of more open water, leads and hence evaporation close to the measurement site (Vihma, Screen et al. 2016).This difference in moisture content could also affect the simulated temperature, e.g., due to the impact on cloud formation.

As mentioned before, the simulated peak of 3.5 ppbv value for the DMS mixing ratio value has not been observed in the Arctic before (Mungall, Croft et al. 2016, Abbatt, Leaitch et al. 2018). The simulated DMS concentrations could not be validated due to the lack of observation during the Arctic- ICE campaign. This highlights the need for concurrent atmospheric DMS measurements when having such a campaign focussing on ocean-sea ice DMS cycling but this study has already clearly shown how sensitive simulated DMS mixing ratios are to the representation of boundary layer mixing and chemistry stressing the need to also include these features in follow- up experimental and modelling studies of Arctic DMS cycling.

6. Conclusion and Recommendations

In the Arctic, enhanced warming may have implications for climate active trace gas exchange in the region. This could in turn affect Arctic climate and hence needs to be well understood. The upcoming MOSAiC project is a scientific effort to help improve this understanding through measurements and modelling. In this study, also being a preparatory study for the measurement and modelling component of the project with a focus on climate-active trace gas exchange, we used a literature review and identified the relevant biogeochemical and physical processes involved in DMS and CO_2 production and consumption in the Arctic. We find that the main source and sink terms have been largely identified but our understanding is not complete. For example, little is known about the activity of the DMSP-lyase enzyme and the impact of the changing Arctic climate on the DMS production. There is also uncertainty in their representation in models due to lack of in-situ measurements. For example, bacterial consumption of DMSPd/DMS, grazing rates of zooplankton have not been measured in the Arctic.

Additionally, we also used a combination of a more process-based model of sea-ice and ocean DMS cycling and a 1-D meteorological and chemistry model (SCM) to simulate DMS cycling in sea ice /ocean and atmosphere, respectively. The sea-ice and ocean DMS cycle model implemented in SMART resulted in simulated DMS/DMSP concentrations and fluxes comparable to the original model analysis by Hayashida, Steiner et al. (2017) but showed different temporal variability. Furthermore, the release of DMS from the underlying water column into the atmosphere varied by season, with the highest fluxes of ~3.4 µmol m^{-2} d^{-1} in the first week of July which was lower than that reported by Hayashida et al., (2017). These discrepancies can be explained due to the use of prescribed data, constant parameters and parametrizations of the processes in the model.

The maximum DMS mixing ratio values simulated by the SCM were 3-5 ppbv, in late Spring with very shallow boundary layer depth. These unrealistically high values could not be corroborated due to missing measurements of DMS mixing ratios from the Arctic-ICE campaign and details on specific features such as a very shallow inversion layer. Furthermore, the wind speed and temperature values were also underestimated by the model. This could be attributed to the representativeness of the ECMWF data that was used to nudge the SCM. In a sensitivity analysis aiming to enhance mixing in the boundary layer, the mixing ratio values reached ~9 ppbv, which were higher than before and in contrast to our expectations. We then evaluated the oxidants mixing ratios and found them to be substantially smaller compared to the reference simulation. This indicated reduced oxidation of DMS and a possible explanation for the simulated high mixing ratios values. Hence, there is a need to consider several meteorological and chemical oxidation processes to understand the role of DMS in the Arctic.

From this study we can conclude that, our understanding of DMS in the Arctic has improved in the recent years but several processes are yet to be measured, parameterized and included in physical, atmospheric and biogeochemical models. In order to understand the cycling of DMS, all the parameters in the sea ice, underlying water and atmosphere need to be measured within the same time period. This is the knowledge gap that the MOSAiC campaign will help to reduce, through the year-long measurements of the several process. This holistic approach will provide a large amount of data that can be used to deepen our understanding of not only DMS but also the entire Arctic climate.

Recommendations-

For future studies and the MOSAiC campaign, we recommend that-

- DMSPd and DMS concentrations in the sea ice and underlying water column should be measured for long durations, preferentially a full annual cycle, which will enable better quantification of the individual source and sink terms.
- Atmospheric concentrations of DMS and its oxidation products should be measured jointly with detailed observations of micro- and boundary layer meteorological parameters to draw conclusions about its role in Arctic climate.
- Brine convection, bubbling of gases from sea ice, halogen chemistry in the atmosphere etc., need to be estimated from measurement campaigns and should then be included in models to improve their performance.

7. References

(n.d.). "An entire year trapped in the Arctic ice." Retrieved Feburary 11, 2019, from https://www.mosaic-expedition.org.

(n.d.). "Historical Data." Climate - Environment and Climate Change Canada. Retrieved 06 Februrary, 2019, from http://climate.weather.gc.ca/historical_data/search_historic_data_stations_e.html?searchType=stnName&timeframe=1&txtStationName=Resolute+&searchMethod=contains&optLimit=yearRange&StartYear=2010&EndYear=2010&Year=2018&Month=12&Day=11&selRowPerPage=25.

(n.d., 13 February, 2018). "Nudging." Retrieved 4 February, 2019, from http://www.ukca.ac.uk/wiki/index.php/Nudging.

Abbatt, J. P., et al. (2018). "New insights into aerosol and climate in the Arctic." Atmospheric Chemistry and Physics Discussions: (in press).

Aliabadi, A., et al. (2015). "Air quality monitoring in communities of the Canadian Arctic during the high shipping season with a focus on local and marine pollution." Atmospheric Chemistry and Physics **15**(5): 2651-2673.

Anderson, B., et al. (1994). "Summertime tropospheric ozone distributions over central and eastern Canada." Journal of Geophysical Research: Atmospheres **99**(D1): 1781-1792.

Archer, S., et al. (2013). "Contrasting responses of DMS and DMSP to ocean acidification in Arctic waters." Biogeosciences (BG) **10**: 1893-1908.

Arrigo, K. R., et al. (2008). "Impact of a shrinking Arctic ice cover on marine primary production." Geophysical Research Letters **35**(19).

Asher, E. C., et al. (2011). "High concentrations and turnover rates of DMS, DMSP and DMSO in Antarctic sea ice." Geophysical Research Letters **38**(23).

Barnes, E. A. and J. A. Screen (2015). "The impact of Arctic warming on the midlatitude jet-stream: Can it? Has it? Will it?" Wiley Interdisciplinary Reviews: Climate Change **6**(3): 277-286.

Becagli, S., et al. (2016). "Relationships linking primary production, sea ice melting, and biogenic aerosol in the Arctic." Atmospheric environment **136**: 1-15.

Breider, T., et al. (2010). "Impact of BrO on dimethylsulfide in the remote marine boundary layer." Geophysical Research Letters **37**(2).

CarbonTracker, E. (2018). "Summary." Retrieved April 28, 2019, from http://www.carbontracker.eu/summary.html.

Charlson, R. J., et al. (1987). "Oceanic phytoplankton, atmospheric sulphur, cloud albedo and climate." Nature **326**(6114): 655.

Cheng-Ying, D., et al. (2011). "Analysis of atmospheric boundary layer height characteristics over the Arctic Ocean using the aircraft and GPS soundings." Atmospheric and Oceanic Science Letters **4**(2): 124-130.

Coumou, D., et al. (2018). "The influence of Arctic amplification on mid-latitude summer circulation." Nature communications **9**(1): 2959.

Cox, C. J., et al. (2015). "Humidity trends imply increased sensitivity to clouds in a warming Arctic." Nature communications **6**: 10117.

Cropp, R., et al. (2007). "Dimethylsulphide, clouds, and phytoplankton: Insights from a simple plankton ecosystem feedback model." Global Biogeochemical Cycles **21**(2).

Delille, B., et al. (2014). "Southern Ocean CO2 sink: The contribution of the sea ice." Journal of Geophysical Research: Oceans **119**(9): 6340-6355.

Fer, I. and K. Widell (2007). "Early spring turbulent mixing in an ice-covered Arctic fjord during transition to melting." Continental Shelf Research **27**(15): 1980-1999.

Ferek, R. J., et al. (1995). "Dimethyl sulfide in the arctic atmosphere." Journal of Geophysical Research: Atmospheres **100**(D12): 26093-26104.

Flato, G. M. and R. D. Brown (1996). "Variability and climate sensitivity of landfast Arctic sea ice." Journal of Geophysical Research: Oceans **101**(C11): 25767-25777.

Francis, J. A. and S. J. Vavrus (2012). "Evidence linking Arctic amplification to extreme weather in mid-latitudes." Geophysical Research Letters **39**(6).

Fransson, A., et al. (2017). "Effects of sea-ice and biogeochemical processes and storms on under-ice water fCO2 during the winter-spring transition in the high Arctic Ocean: Implications for sea-air CO2 fluxes." Journal of Geophysical Research: Oceans **122**(7): 5566-5587.

Galindo, V., et al. (2014). "Biological and physical processes influencing sea ice, under-ice algae, and dimethylsulfoniopropionate during spring in the Canadian Arctic Archipelago." Journal of Geophysical Research: Oceans **119**(6): 3746-3766.

Ganzeveld, L., et al. (2010). "Impact of future land use and land cover changes on atmospheric chemistry-climate interactions." Journal of Geophysical Research: Atmospheres **115**(D23).

Ganzeveld, L., et al. (2008). "Surface and boundary layer exchanges of volatile organic compounds, nitrogen oxides and ozone during the GABRIEL campaign." Atmospheric Chemistry and Physics **8**(20): 6223-6243.

Ganzeveld, L., et al. (2002). "Global soil-biogenic NOx emissions and the role of canopy processes." Journal of Geophysical Research: Atmospheres **107**(D16).

Ghahremaninezhad, R., et al. (2017). "Boundary layer and free-tropospheric dimethyl sulfide in the Arctic spring and summer." Atmospheric Chemistry and Physics **17**(14): 8757-8770.

Golden, K., et al. (1998). "The percolation phase transition in sea ice." Science **282**(5397): 2238-2241.

Gosink, T. A., et al. (1976). "Gas movement through sea ice." Nature **263**(5572): 41.

Gradinger, R. (2009). "Sea-ice algae: Major contributors to primary production and algal biomass in the Chukchi and Beaufort Seas during May/June 2002." Deep Sea Research Part II: Topical Studies in Oceanography **56**(17): 1201-1212.

Halloran, P., et al. (2010). "Can we trust empirical marine DMS parameterisations within projections of future climate?" Biogeosciences **7**(5): 1645-1656.

Hayashida, H., et al. (2017). "Implications of sea-ice biogeochemistry for oceanic production and emissions of dimethyl sulfide in the Arctic." Biogeosciences **14**(12): 3129-3155.

Hoffmann, E. H., et al. (2016). "An advanced modeling study on the impacts and atmospheric implications of multiphase dimethyl sulfide chemistry." Proceedings of the National Academy of Sciences **113**(42): 11776-11781.

Hopkins, F. E., et al. (2018). "Dimethylsulfide (DMS) production in polar oceans is resilient to ocean acidification." Biogeosciences Discussions.

Hudson, E., et al. (2001). "Weather of Nunavut and the Arctic." NAV Canada, Ottawa, Ontario.

Kiene, R. P., et al. (2000). "New and important roles for DMSP in marine microbial communities." Journal of Sea Research **43**(3-4): 209-224.

Kim, K.-Y., et al. (2019). "Vertical Feedback Mechanism of Winter Arctic Amplification and Sea Ice Loss." Scientific reports **9**(1): 1184.

Kloster, S., et al. (2006). "DMS cycle in the marine ocean-atmosphere system? a global model study." Biogeosciences Discussions **2**(4): 1067-1126.

Kotovitch, M., et al. (2016). "Air-ice carbon pathways inferred from a sea ice tank experiment." Elementa: Science of the Anthropocene.

Kramer, M. R. and H. Scholten (2001). The Smart approach to modelling and simulation. Delft, The Netherlands, TU Delft.

Kuhn, U., et al. (2010). "Impact of Manaus City on the Amazon Green Ocean atmosphere: ozone production, precursor sensitivity and aerosol load." Atmospheric Chemistry and Physics **10**(19): 9251-9282.

Lavoie, D., et al. (2005). "Modeling ice algal growth and decline in a seasonally ice-covered region of the Arctic (Resolute Passage, Canadian Archipelago)." Journal of Geophysical Research: Oceans **110**(C11).

Leaitch, W. R., et al. (2013). "Dimethyl sulfide control of the clean summertime Arctic aerosol and cloud." Elem Sci Anth **1**.

Lee, P. A., et al. (2001). "Particulate dimethylsulfoxide in Arctic sea-ice algal communities: The cryoprotectant hypothesis revisited." Journal of Phycology **37**(4): 488-499.

Levasseur, M. (2013). Impact of Arctic meltdown on the microbial cycling of sulphur, Nat. Geosci., 6, 691–700.

Li, S. M. and L. A. Barrie (1993). "Biogenic sulfur aerosol in the Arctic troposphere: 1. Contributions to total sulfate." Journal of Geophysical Research: Atmospheres **98**(D11): 20613-20622.

Luce, M., et al. (2011). "Distribution and microbial metabolism of dimethylsulfoniopropionate and dimethylsulfide during the 2007 Arctic ice minimum." Journal of Geophysical Research: Oceans **116**(C9).

Ma, S., et al. (2018). "Polarized Response of East Asian Winter Temperature Extremes in the Era of Arctic Warming." Journal of Climate(2018).

Mahmood, R., et al. (2018). "Sensitivity of Arctic sulfate aerosol and clouds to changes in future surface seawater dimethylsulfide concentrations." Atmospheric Chemistry and Physics Discussions: 1-25.

Moreau, S., et al. (2015). "Drivers of inorganic carbon dynamics in first-year sea ice: A model study." Journal of Geophysical Research: Oceans **120**(1): 471-495.

Mortenson, E., et al. (2017). "A model-based analysis of physical and biological controls on ice algal and pelagic primary production in Resolute Passage." Elem Sci Anth **5**.

Motard-Côté, J., et al. (2012). "Distribution and metabolism of dimethylsulfoniopropionate (DMSP) and phylogenetic affiliation of DMSP-assimilating bacteria in northern Baffin Bay/Lancaster Sound." Journal of Geophysical Research: Oceans **117**(C9).

Mundy, C. J., et al. (2014). "Role of environmental factors on phytoplankton bloom initiation under landfast sea ice in Resolute Passage, Canada." Marine Ecology Progress Series **497**: 39-49.

Mungall, E. L., et al. (2016). "Dimethyl sulfide in the summertime Arctic atmosphere: measurements and source sensitivity simulations." Atmospheric Chemistry and Physics **16**(11): 6665-6680.

Nomura, D., et al. (2006). "The effect of sea-ice growth on air–sea CO2 flux in a tank experiment." Tellus B: Chemical and Physical Meteorology **58**(5): 418-426.

Papadimitriou, S., et al. (2004). "Experimental evidence for carbonate precipitation and CO2 degassing during sea ice formation." Geochimica et Cosmochimica Acta **68**(8): 1749-1761.

Park, K. T., et al. (2018). "Atmospheric DMS in the Arctic Ocean and its relation to phytoplankton biomass." Global Biogeochemical Cycles **32**(3): 351-359.

Parmentier, F.-J. W., et al. (2013). "The impact of lower sea-ice extent on Arctic greenhouse-gas exchange." Nature climate change **3**(3): 195.

Roelofs, G. J., et al. (1998). "Simulation of global sulfate distribution and the influence on effective cloud drop radii with a coupled photochemistry sulfur cycle model." Tellus B **50**(3): 224-242.

Schwinger, J., et al. (2017). "Amplification of global warming through pH dependence of DMS production simulated with a fully coupled Earth system model." Biogeosciences **14**: 3633-3648.

Semiletov, I., et al. (2004). "Atmospheric CO2 balance: The role of Arctic sea ice." Geophysical Research Letters **31**(5).

Seok, B., et al. (2013). "Dynamics of nitrogen oxides and ozone above and within a mixed hardwood forest in northern Michigan." Atmospheric Chemistry and Physics **13**: 7301.

Serreze, M. C. and J. A. Francis (2006). "The Arctic amplification debate." Climatic change **76**(3-4): 241-264.

Sharma, S., et al. (2012). "Influence of transport and ocean ice extent on biogenic aerosol sulfur in the Arctic atmosphere." Journal of Geophysical Research: Atmospheres **117**(D12).

Simó, R. and C. Pedrós-Alió (1999). "Role of vertical mixing in controlling the oceanic production of dimethyl sulphide." Nature **402**(6760): 396.

Søren, R., et al. (2011). "Sea ice contribution to the air–sea CO2 exchange in the Arctic and Southern Oceans." Tellus B: Chemical and Physical Meteorology **63**(5): 823-830.

Stefels, J., et al. (2012). "The analysis of dimethylsulfide and dimethylsulfoniopropionate in sea ice: Dry-crushing and melting using stable isotope additions." Marine chemistry **128**: 34-43.

Stefels, J., et al. (2007). "Environmental constraints on the production and removal of the climatically active gas dimethylsulphide (DMS) and implications for ecosystem modelling." Biogeochemistry **83**(1-3): 245-275.

Stefels, J., et al. (2018). "Impact of sea-ice melt on dimethyl sulfide (sulfoniopropionate) inventories in surface waters of Marguerite Bay, West Antarctic Peninsula." Phil. Trans. R. Soc. A **376**(2122): 20170169.

Steiner, N., et al. (2016). "What sea-ice biogeochemical modellers need from observers." Elem Sci Anth **4**.

Steiner, N., et al. (2006). "Simulating the coupling between atmosphere–ocean processes and the planktonic ecosystem during SERIES." Deep Sea Research Part II: Topical Studies in Oceanography **53**(20-22): 2434-2454.

Taalba, A., et al. (2013). "Photooxidation of dimethylsulfide (DMS) in the Canadian Arctic." Biogeosciences **10**(11): 6793-6806.

Tedesco, L. and M. Vichi (2014). "Sea ice biogeochemistry: A guide for modellers." PloS one **9**(2): e89217.

Tison, J.-L., et al. (2002). "Tank study of physico-chemical controls on gas content and composition during growth of young sea ice." Journal of Glaciology **48**(161): 177-191.

Tjernstrom, M., et al. (2012). "Meteorological conditions in the central Arctic summer during the Arctic Summer Cloud Ocean Study (ASCOS)." Atmospheric Chemistry and Physics **12**(15): 6863-6889.

Vihma, T., et al. (2016). "The atmospheric role in the Arctic water cycle: A review on processes, past and future changes, and their impacts." Journal of Geophysical Research: Biogeosciences **121**(3): 586-620.

Vihma, T., et al. (2018). "Towards the Marine Arctic Component of the Pan-Eurasian Experiment." Atmos. Chem. Phys. Discuss.

Yang, Y., et al. (2018). "Sulfate aerosol in the Arctic: Source attribution and radiative forcing." Journal of Geophysical Research: Atmospheres **123**(3): 1899-1918.

Yasunaka, S., et al. (2018). "Arctic Ocean CO 2 uptake: an improved multiyear estimate of the air–sea CO 2 flux incorporating chlorophyll a concentrations." Biogeosciences **15**(6): 1643-1661.

Zhou, J., et al. (2013). "Physical and biogeochemical properties in landfast sea ice (Barrow, Alaska): Insights on brine and gas dynamics across seasons." Journal of Geophysical Research: Oceans **118**(6): 3172-3189.

8. Appendix

8.1.Tables

Table 1 Parameter values used in SMART model implementation from Hayashida et al.,2017, when different Hayashida values are given in parentheses.

Parameter	**Identity**	**Value (Hayashida values)**	**Unit**	**Reason for difference with Hayashida et al.,2017**
Initial value of DMSPd	DMSPd0	0.1	nmol L^{-1}	-
Initial value of DMS	DMS0	0.1	nmol L^{-1}	-
Initial value of ice algae concentration	IA0	8.0		
Melt pond drainage	rmp	0.0175	md^{-1}	-
Active exudation fraction	factive, fp1active, fp2active	0.05,0.05,0.05	-	-
Sloppy feeding fraction	fz1sloppy, fz2sloppy	0.3,0.3	-	-
Bacterial yield	fyield, fwcyield*	0.2,0.09 (0.2, 0.2)	-	Model calibration; Values ranging from 0.04-0.3 have been reported for Arctic waters (Luce, Levasseur et al. 2011, Motard-Côté, Levasseur et al. 2012)
Thickness of biologically active layer	hbi	0.03	m	-
Photolysis half-saturation constant	hphotolysis, hwcphotolysis*	1,1	Wm^{-2}	-
Thickness of uppermost layer of water column	hzo	1	m	-
Bacterial DMS consumption rate	kdms, kwcdms*	0.2,0.5	d^{-1}	-
Bacterial DMSPd consumption rate constant	kdmspd, kwcdmspd*	1, 5.5 (1,5)	d^{-1}	Model calibration; Reported values range from 1. -4.1 (Hayashida, Steiner et al. 2017)
Free DMSP-lyase rate constant	kfree, kwcfree*	0.04,0.02 (0.02,0.02)	d^{-1}	Model calibration, 0.04 has been used in (Steiner, Denman et al. 2006)
Cell lysis rate constant	klysis, kp1lysis*, kp2lysis*	0.03, 0.03, 0.03	d^{-1}	-
Photolysis rate constant	kphotolysis, kwcphotolysis*	0.085, 0.1 (0.1,0.1)	d^{-1}	Model Calibration; Values ranging between 0.01-0.11 reported for Canadian Arctic (Taalba, Xie et al. 2013)
Intracellular DMSP-to Chl a ratio	q, qp1*, qp2*	9.5,9.5,9.5 (9.5,100,9.5)	nmol S : µg Chl a	Model calibration, hence our model doesn't differentiate between small and large phytoplankton
Sea ice density	dice	913	kg m^{-3}	-
Sea ice density in equivalent meltwater	dmw	1000	kg m^{-3}	-

Constants used to represent process modelled by physical / ocean ecosystem model in Hayashida et al.,2017				
Melt-pond area fraction	Amp	0.3	-	Calculated by physical model
Transfer velocity	tf	0.0001	-	Model calibration; Highly simplified representation of transfer velocity of flushing; Calculated by the physical model
Phytoplankton growth rate	up1, up2	0.5, 0.5	-	Obtained from specific algal growth rate by Steiner, Denman et al. (2006); Calculated by ocean ecosystem module
Loss rates of small and large phytoplankton due to grazing by zooplankton	Rz1p1, Rz2p2	0.0256	µg Chl a L^{-1} d^{-1}	Obtained from Cropp, Norbury et al. (2007); Calculated by ocean ecosystem model
Vertical diffusivity constant	Kz	10^{-3}	m^2 s^{-1}	Obtained from Fer and Widell (2007); Calculated by physical model
Kronecker's delta	K	1	-	Calculated physical model

*value of parameters for underlying water column

Table 2 List of tabulated parameters used in SMART model along with sources of data

Parameter	Identity	Unit	Source
Radiation	Radtab	Wm^{-2}	SCM model run
Temperature	Tzo	°C	SCM Model run
Wind speed (10m)	U10	ms^{-1}	SCM Model run
Fraction of open water	fowtab	-	SCM model run
Sea ice thickness	TSItab	m	Hayashida et al., 2017
Ice algae concentration	IAtab	µg Chl a L^{-1}	Hayashida et al., 2017
Ice algae growth rate	utab	d^{-1}	Lewis et al., 2018
Nutrient Limitation Index for sea ice	Lnuttab	-	Mortenson et al.,2017
Phytoplankton concentration in water column	Ptab	µg Chl a L^{-1}	Hayashida et al., 2017
Nutrient Limitation Index for water column	Lnutwc_tab	-	Nitrate + Nitrite concentrations obtained from Mundy et al., 2014 and then Lnut calculated using equation 19 in Appendix of Mortenson et al., 2017

8.2. Figures

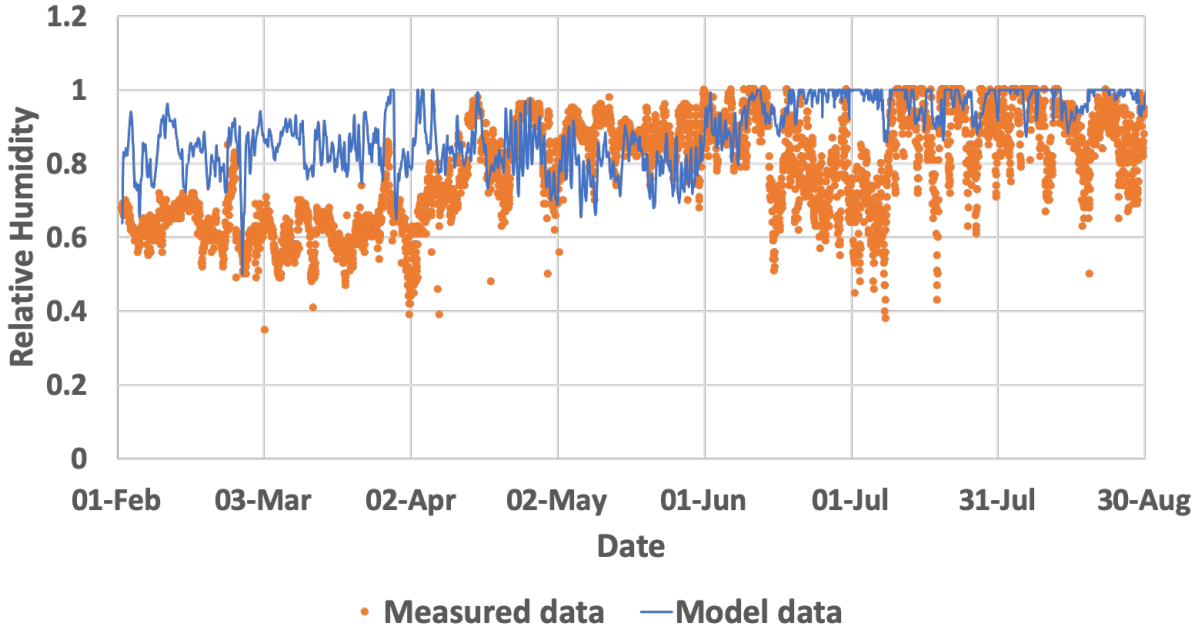

Figure 1 Simulated relative humidity from SCM (blue) and measured at Resolute Airport (orange dots) between 1 February- 1 September, 2010.

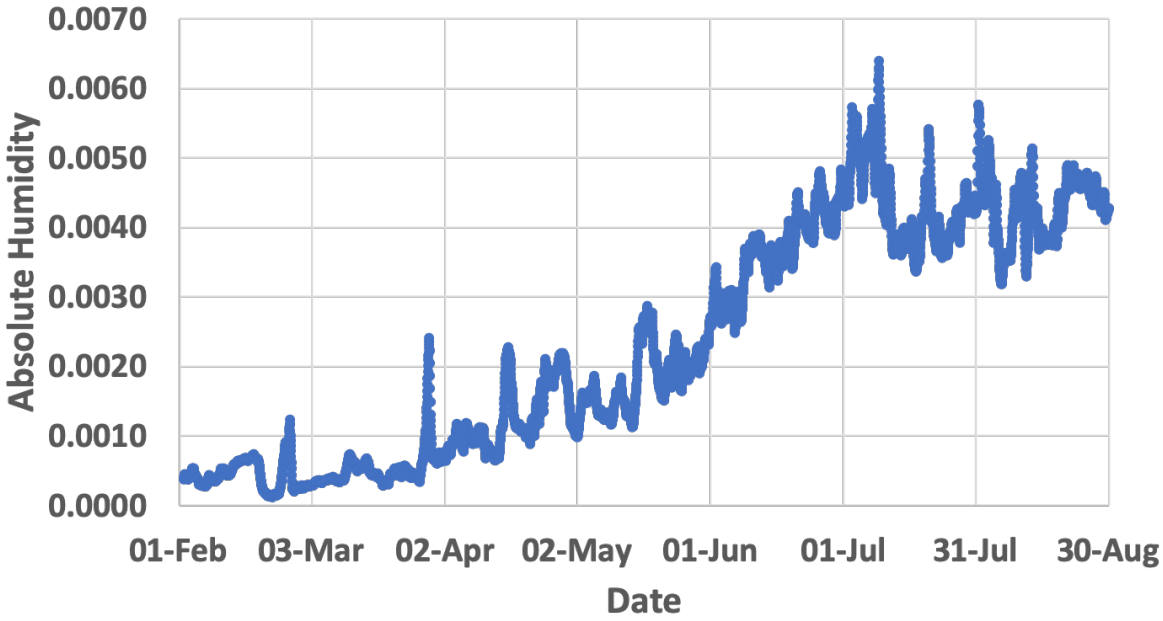

Figure 2 Simulated absolute humidity from SCM (blue) and measured at Resolute Airport (orange dots) from 1 Feb-30 Aug,2010.

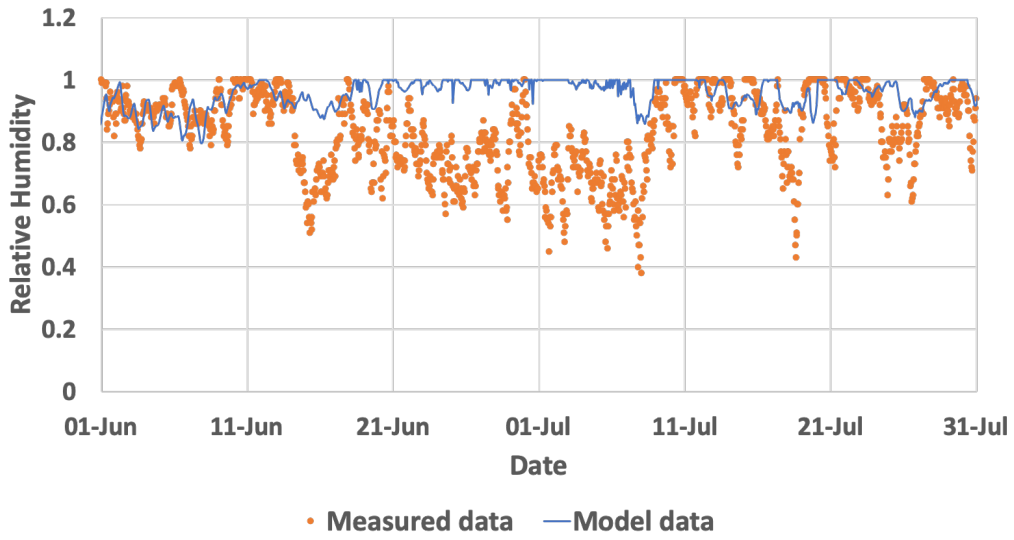

Figure 3 Simulated relative humidity from SCM (blue) and measured at Resolute Airport (orange dots) between 1 June-31 July, 2010.

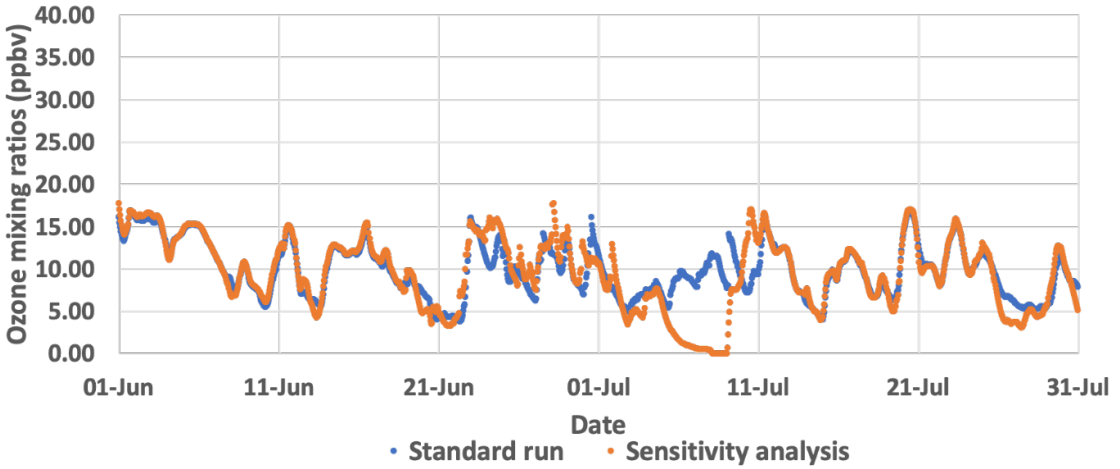

Figure 4 Ozone mixing ratios obtained from SCM model up for the lower 8m height for sensitivity analysis run (Ri=0) from 1 June - 31 July, 2010 along with standard run Ozone mixing ratios.

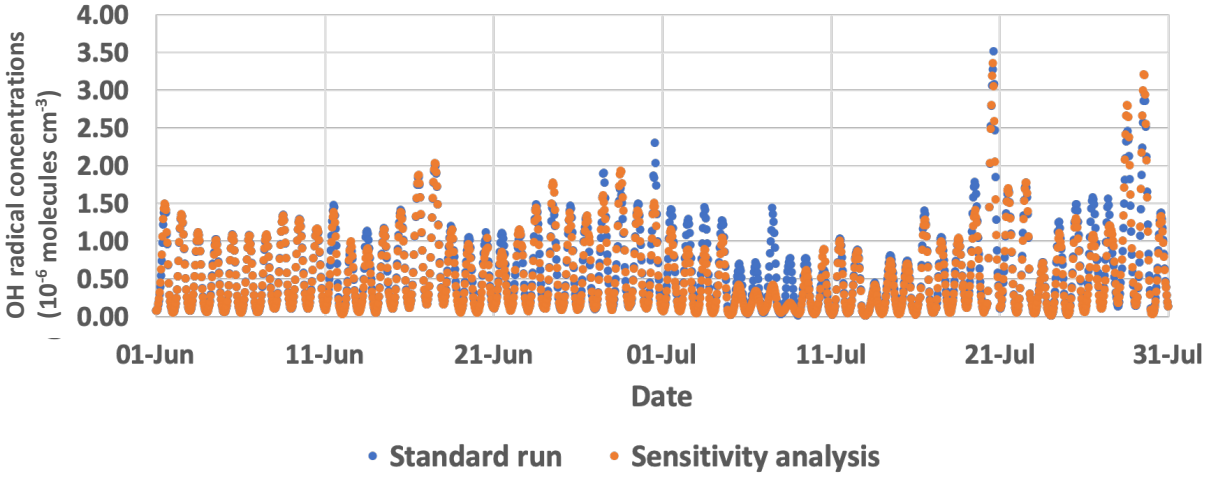

Figure 5 OH^- radical mixing ratios obtained from SCM model up to 800m height for sensitivity analysis run (Ri=0) from 1 June - 31 July, 2010.